Chapter 14: Maps of Volcanogenic Structures

EXTRUSIVE IGNEOUS rocks reach the surface through vents in the Earth's crust, which conduct the eruption of gases, volcanic bombs, ashes, and hot lava. Geological maps of volcanic fields document the spatial distribution of individual lava flows, mudflows, and pyroclastic and epiclastic deposits. Field investigations have revealed that many extrusion vents follow fissure systems, sometimes marked on the ground by an array of closely spaced cinder cones aligned over the fissure zones. Other extrusions built up large shield volcanoes and stratovolcanoes by episodic eruption through subcircular vents. Renewed eruption of such volcanoes commonly involves explosive fracturing and gravity collapse and may create craters and calderas. This chapter includes examples of geological maps of volcanogenic structures and deposits and explains some of the basic features necessary for an elementary understanding of such maps.

Content: Some exploitation purposes of volcanic deposits are discussed in section 14-1. The structure of the ocean floor is illustrated in section 14-2. Flood basalts, shield volcanoes, and stratovolcanoes are outlined in sections 14-3 through 14-5. The map patterns of mudflows and glowing avalanches are illustrated in sections 14-6 and 14-7. Craters, calderas, and eroded volcanic landforms are discussed in section 14-8 and 14-9.

14-1 Exploitation of volcanic rocks

Volcanic eruptions may occur quite unexpectedly, and various estimates suggest that such eruptions have killed, at least, a quarter million people over the past millenium. Much of the destruction is caused, not by the ejected material, but by secondary effects. These effects include: flood waves (tsunamis), caused by the collapse of marine volcanoes; famine due to the spoilage of crops after ashfall; and mudflows, released either by melting of ice sheets on high volcanic cones or by the emptying of crater lakes.

Although volcanoes pose an awesome hazard to man and his construction, they do provide some

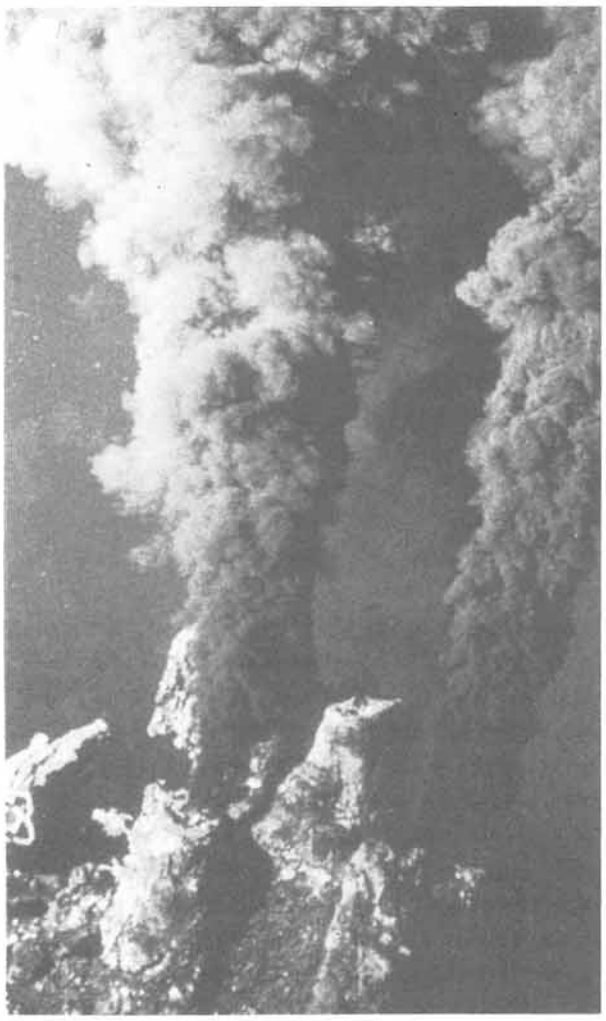

Figure 14-1: "Black smoker" or submarine geyser pours 350° centigrade water, saturated with metallic sulfides, into the cold Pacific waters 2.5 kilometers below sea level. Image taken by French submersible Cyana, 1982, at 13° NL on the mid-Pacific ridge axis.

beneficial products. Extrusive igneous rocks have been used by ancient man for the construction of hunting tools (obsidian), cement, and building stones. Pumice is used as a bathing stone for removing excess callus from footsoles and handpalms. Basalt provides massive masonry. For example, the extensive network of sea dikes in the Netherlands is reinforced with heavy basalt blocks, imported from abroad. The national heritage city of Cappodocia, Turkey, is a magnificent landscape of small conical hills of differentially eroded volcanic ashflows, that were excavated to host houses. The gigantic heads of Easter Island, stoically staring out over the ocean, consist of volcanic pyroclastics. They were sculpted by a people vanished long ago. Volcanic ashes commonly fertilize agricultural land, and the 1912 eruption of Katmai-Novarupta, Alaska, has been quoted as "the best thing that ever happened to Kodiak." Many fine French wines and champagne come from vineyards situated on volcanic soils.

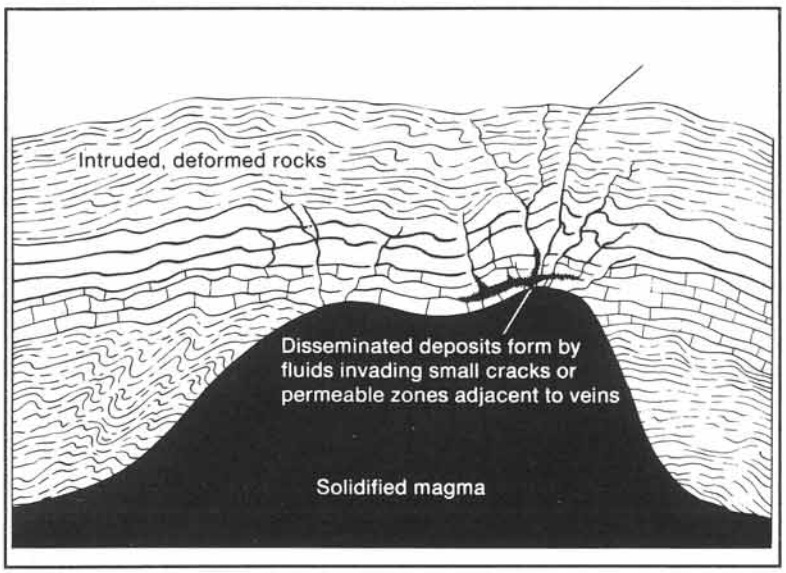

Modern interest in volcanic terrains partly stems from the search for mineral and energy resources. Economic mineral deposits of galena, sphalerite, pyrite, gold, silver, zinc, uranium, and diamonds all are associated with volcanic rocks. Metal-rich sulfide deposits have been formed and are forming today from saturated

Figure 14-2: Pegmatite veins intrude into fissures, emanating from a magma chamber. Other hydrothermal deposits accumulate in the rocks, fractured by the pressure of the central batholith.

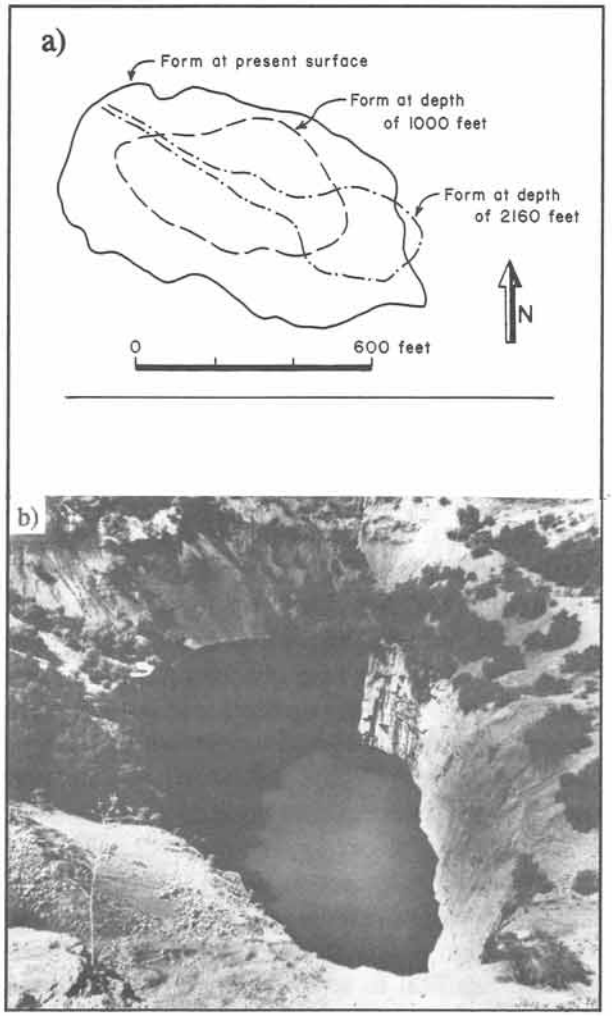

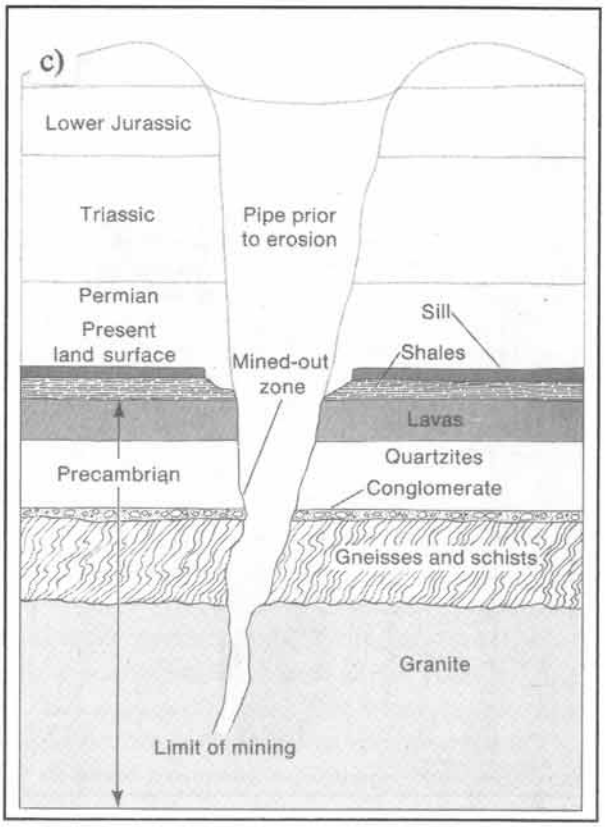

Figure 14-3: *Magma pipe of diamond-bearing kimberlite at Kimberley, South Africa. a) Map projection of pipe outline at three different levels. b) Oblique view into the mined magma pipe. c) Schematic cross-section of the magma pipe up to three kilometers below the ground surface.*

thermal water, rising in "*black smokers*." These are submarine geysers, occurring along the axial fracture zone of active mid-oceanic ridges, ejecting hot water that precipitates massive sulfide deposits upon mixture with the ambient, cold sea water (Fig. 14-1).

Other important ore bodies are found near subvolcanic complexes, formed by hydrothermal fluids, rising through fractures in the host rock. The solutions scavenge particular elements from the country rock to precipitate elsewhere in lead, zinc, and gold-bearing quartz veins (Fig. 14-2). Subvolcanic stocks of ultrabasic, high-pressure magmas or *kimberlites* carry up diamonds from over 200 kilometers deep and are mined extensively in South Africa. The prototype diamond pipe at Kimberley, South Africa, was mined to over one-kilometer depth.It follows a fissure in the subsurface but concentrates into a funnel shape of subcircular plan-section near the surface (Fig. 14-3a & b). The upward widening suggests that pressure was such that, on approaching the surface, an extensive blow-out occurred to form a conical pipe and pyroclastic deposits. Steep-sided pipes of igneous origin are, also, called *stocks*, *plugs*, *necks*, or *diatremes*. Deep circular surface depressions associated with blow-outs are termed *maars* (Fig. 14-3c).

The residual *geothermal energy* in the subsurface of recent and subrecent volcanic regions has

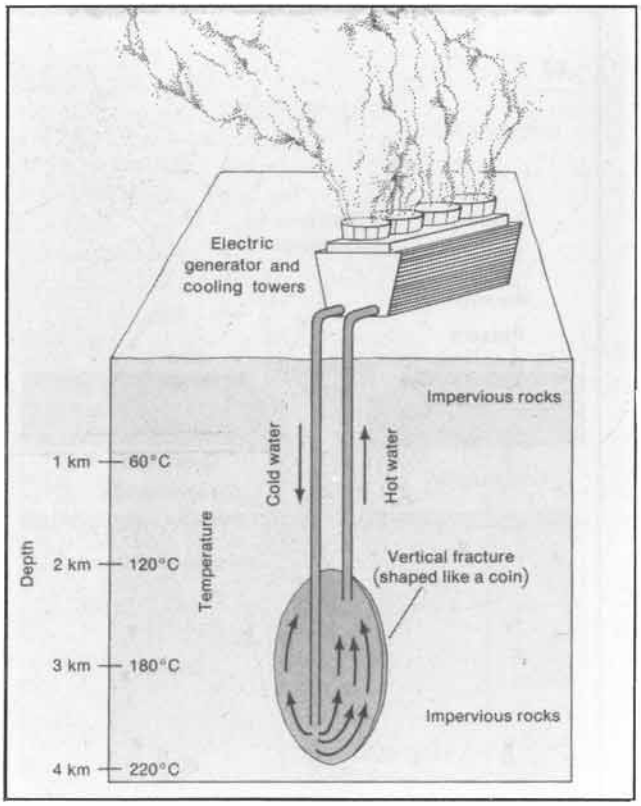

Figure 14-4: *Fractures in hot igneous rocks can be injected with water to extract geothermal energy for heating purposes and the generation of electricity. Illustrated is a region with a steep geothermal gradient of 60° centigrade per kilometer.*

been exploited in ancient times by the Romans and Arabs for the heating of elaborate public bath houses. The natural steam eruptions or geysers of Iceland and Old Faithful in Yellowstone National Park, Wyoming, are major tourist attractions. Modern man extracts geothermal energy for municipal waterworks on a grand scale (Fig. 14-4). For example, all of Iceland's houses, offices, schools, and greenhouses (for its domestic banana production and consumption) are heated by geothermal steam and hot water pipes. Large extractions, also, occur in Italy, New Zealand, Kenya, and Hawaii, with much room for expansion in other developing countries, such as the Philippines and Indonesia.

14-2 Ocean floor

Geoscientists have pieced together a picture of plate tectonic evolution, involving the breakup, dispersal, and renewed aggregation of *supercontinents*. Presently, at least a dozen major plates are distinguished. This book concentrates on the methods of geological map interpretation and avoids a detailed treatment of plate tectonics, which is already covered in other texts. But the movement of tectonic plates continually renews our ocean floors, which are covered with extensive basalt flows.

The tectonic plates are formed by dispersal of the continental fragments and accretion of new oceanic lithosphere. Pangea, the Earth's youngest single supercontinent, broke up about 200 million years ago. The age distribution of the ocean floor is outlined in Figure 14-5 in transverse Hammer-Aitoff projection. This projection gives an overview of the oceanic spreading pattern in a single map by placing the South Pole in the central node and the north polar axis at the top.

The rifting and tearing apart of continental crust continues at present, as the mid-oceanic rift of the Indian Ocean propagates northward into the Red Sea arm to separate further the Arabian plate from the African plate. The opening of new oceans is compensated for by the closure of other oceans. The global production and consumption of oceanic lithosphere occurs at rates ranging between 2.4 and 3.5 centimeters per year. The mid-Atlantic ridge spreads at a time-averaged rate of about three centimeters per year.

Iceland is located on the mid-Atlantic spreading ridge - the western half is part of the North American plate and the eastern half part of the Eurasian plate. Volcanic eruptions, associated with the growth of the island, are extremely frequent. The Surtsey volcano formed between 1963 and 1967 close to the southwest coast of Iceland by an outpouring of one cubic kilometer of ash and lava (Fig. 14-6). Surtsey is the southwesternmost of the Vestmann Islands, which all lie along a branch of the mid-Atlantic rift zone.

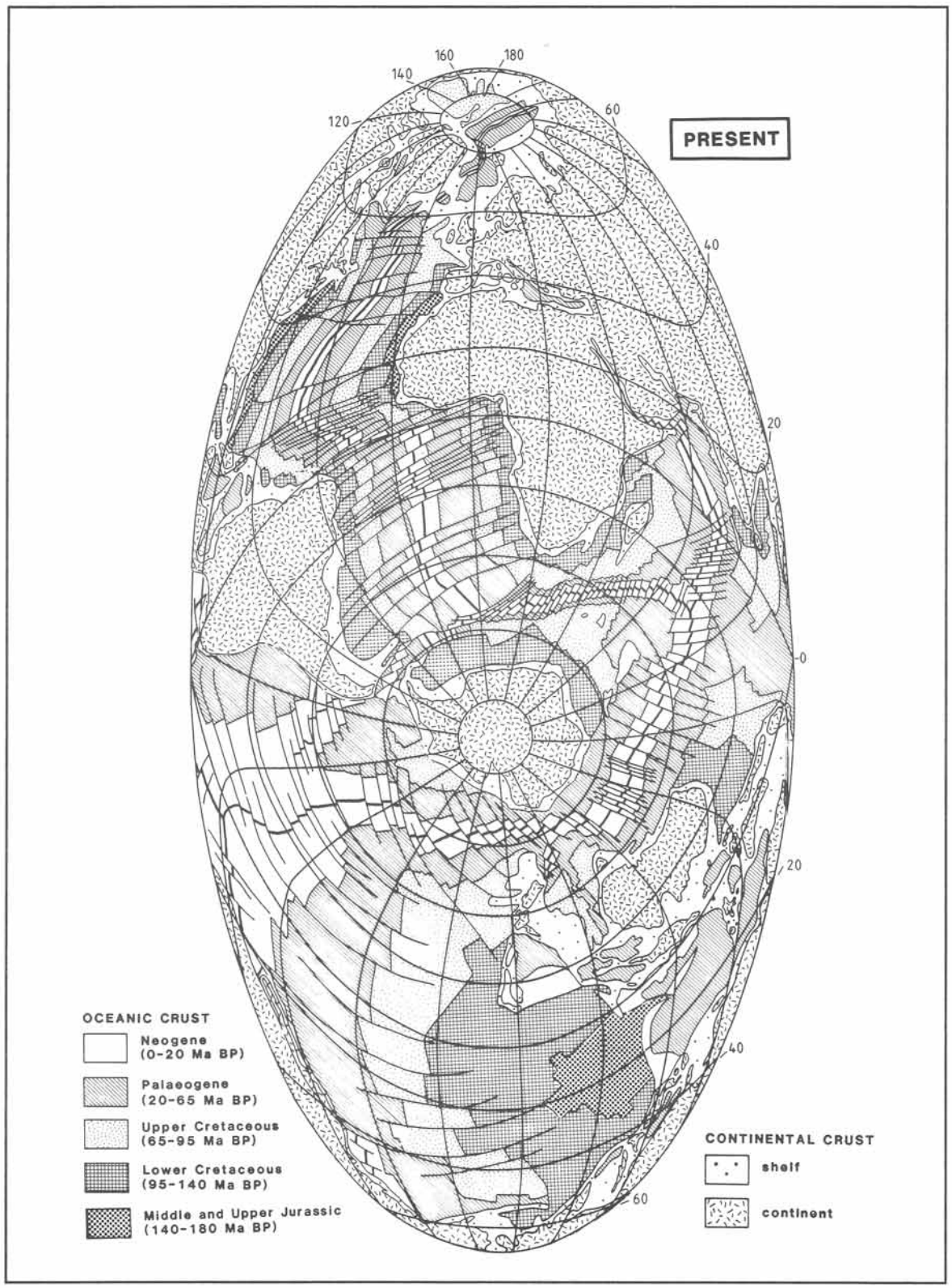

Figure 14-5: *Age distribution of the basaltic ocean floor in transverse Hammer-Aitoff projection.*

14-3 Flood basalts

Zones of incipient rifting are characterized by the intrusion of basic dikes. Progressive extension may lead to complete failure of the continental crust, accompanied by extrusion of basaltic lavas and the formation of oceanic crust. Continental rifting first produces basalts of the alkali magma series (alkali olivine basalts). It is only after the continental separation that the ocean floor crust of tholeiitic basalt forms. However, not all fractures in the continental crust succeed to form a separate plate boundary; these are the *failed rift-arms* or *aulacogens*. They are marked by dikes of alkali basalt, some of which manage to pour out large volumes of basaltic lavas onto the surface; these deposits are known as *flood basalts*. Figure 14-7 illustrates the breakup of Gondwana, some 140 million years ago, and outlines the regions where thick plateaus of stacked basalt flows have accumulated in Jurassic and Cretaceous rift zones. Continental alkali-basalts commonly contain more sodium and potassium than is typical for basalts of the ocean floor, which are not contaminated by partial melts of the sialic continental crust.

The progressive build-up of plateaus of flood basalts is continuing at present. Cenozoic basalts episodically erupt from fissures, splaying away from the opening Red Sea. The fissure system includes the aborted spreading zones of the African rift valley, Afar triangle, Danakil depression, and tears in the Arabian Peninsula (Fig. 14-8). Flood basalts typically are fissure eruptions, and the subrecent lava fields of the western province of Saudi Arabia have emanated from *en-echelon fractures*, splaying away from the Red Sea rift in what is referred to as the Makkah-Madinah-Nafud volcanic line (Fig. 14-9). Such fissure zones are commonly marked at the surface by a series of aligned *spatter cones* and *cinder cones* (Fig. 14-10a & b). Cinder cones are usually less than 300 meters high and are comprised of steep, 30° to 40° slopes, built from scoriaceous *pyroclastics*, i.e., ejected, airborne lava fragments (Fig. 14-10b). Such pyroclasts sometimes agglutinate into a hard deposit. Figures 14-11a and b are examples of regularly-spaced cinder cones, that mark the one-million-year-old fissure of Harrat Kishb, Saudi Arabia, and similar cones along the

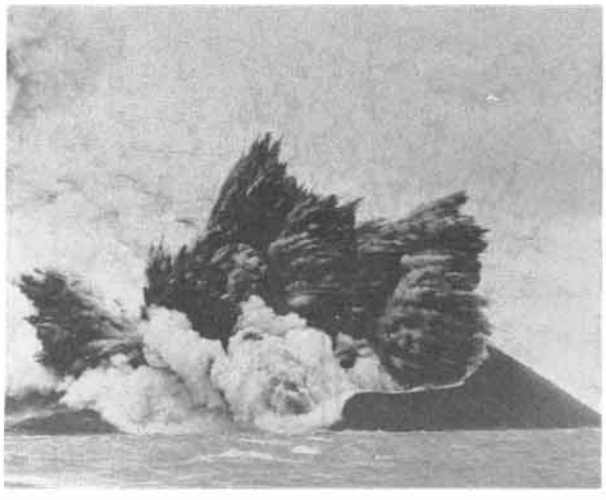

Figure 14-6: *Explosive eruption of Surtsey, Iceland.*

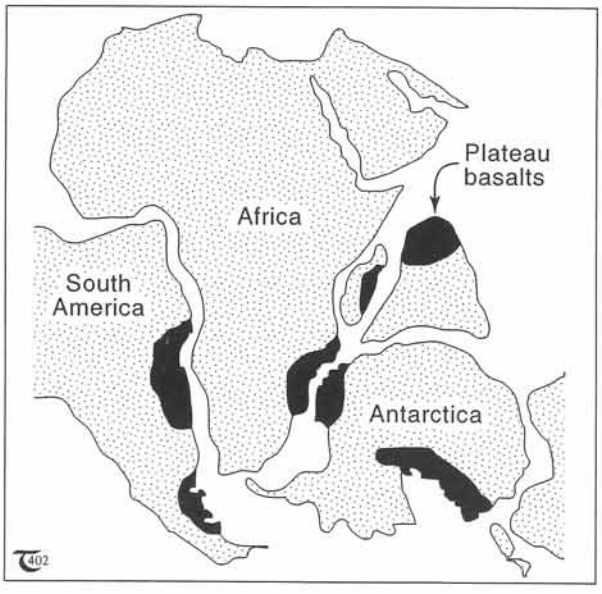

Figure 14-7: *Extent of plateau basalts along rift zones that broke up Gondwana about 140 million years ago. The age of the plateau basalts spans the entire epoch of modern plate movement.*

twenty-kilometer-long Laki fissure of 1783, Iceland. The Laki eruption represents the largest lava flood in recent history and was accompanied by a series of minor earthquakes. The map pattern of the Laki rift and associated cones is quite similar to that of the 2,100-year-old array of cones along the Great Rift Zone of the Craters of the Moon National Monument, Idaho (Fig. 14-12a & b).

A much larger plateau of Miocene flood basalts occupies the Columbia River Plateau, Washington, northwest of the volcanic province of the Craters of the Moon in the Snake River Plain (Fig. 14-13a). The Columbia basalts are locally up to 1,500 meters thick, cover an area of over 130,000 square kilometers, and may have formed in about ten million years. A still larger province of flood basalts occurs in the Deccan Plains, India, where 250,000 square kilometers of Cretaceous basalt lavas rest on the Precambrian basement (Fig. 14-13b). The Deccan *traps* ("steps") are up to two kilometers thick and include individual lava flows, ranging from one to sixty meter thick. The feeder fissures in the older provinces of flood basalts are no longer marked by spatter and scoria cones at the surface, which disappear by erosion in about four million years. But remnants of cinder cones commonly become entrapped within the sequence of flood basalts (Fig. 14-14).

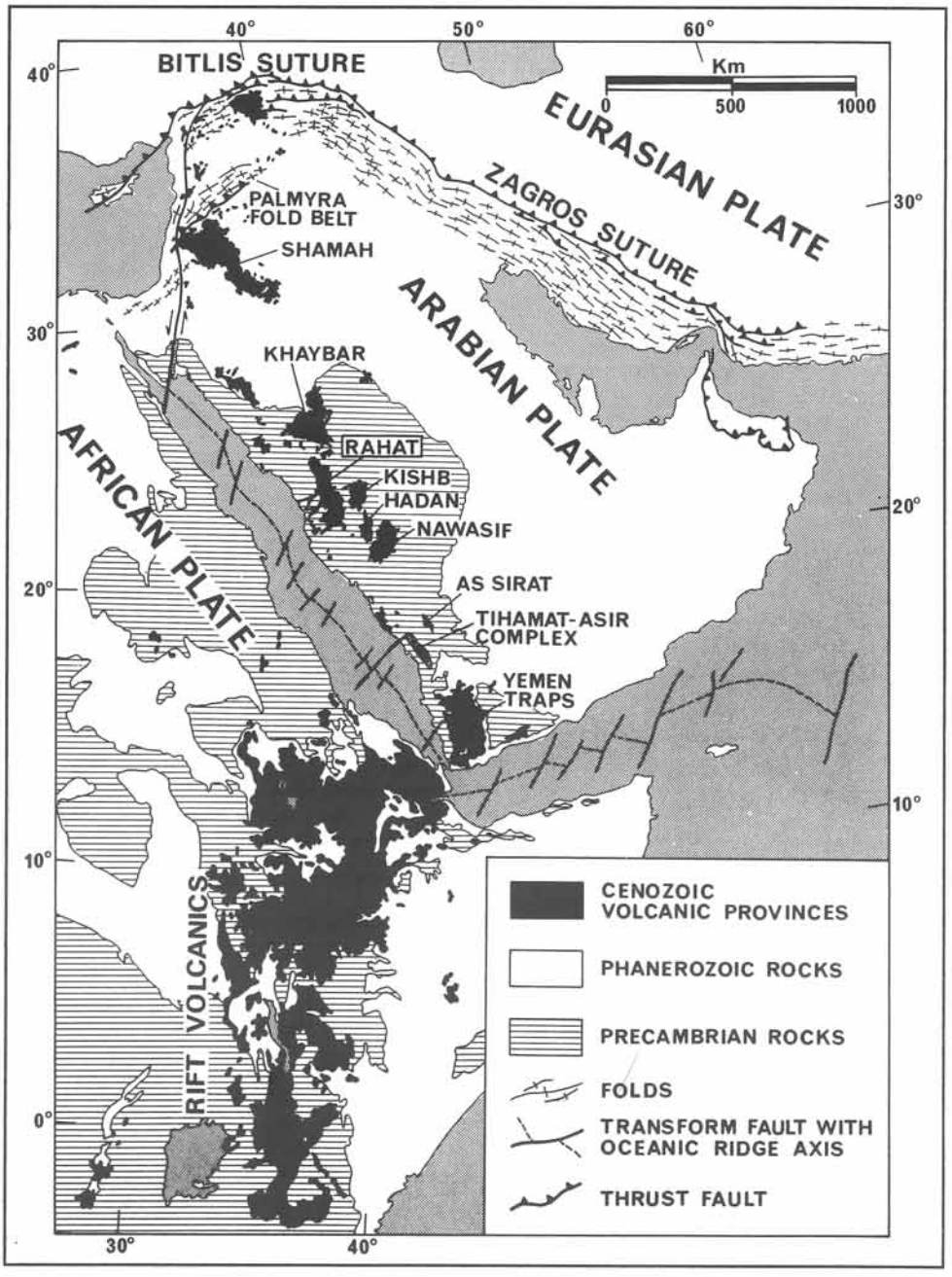

Figure 14-8: *Geological map of territory and recent basalts in the active rift zone of the Red Sea and the East African rift valley.*

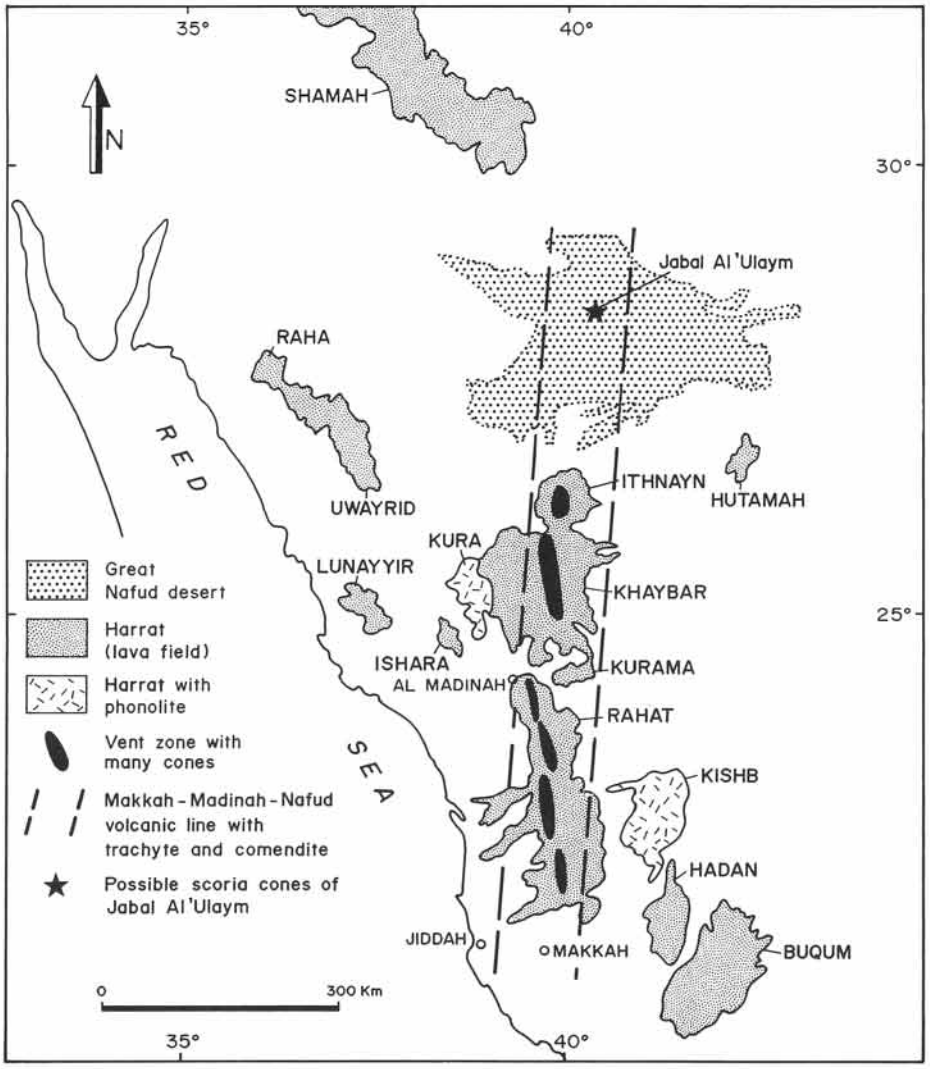

Figure 14-9: *Map of Neogene-Quaternary lava fields in western Arabia. The vent zones mark an en-echelon pattern of fractures, splaying away from the Red Sea rift zone.*

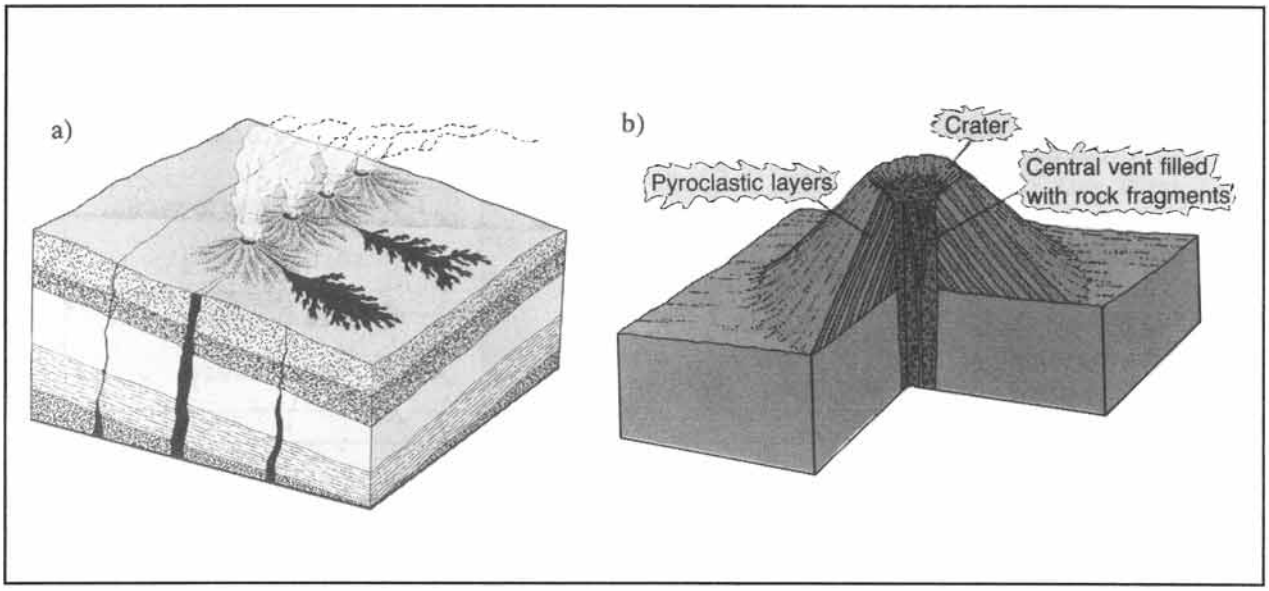

Figure 14-10: *The vent zones that feed flood basalts are commonly marked at the surface by a series of aligned cinder cones, that develop during a late stage in the eruption of each lava flood. a) Block diagram of aligned cinder cones. b) Detail of single cinder cone.*

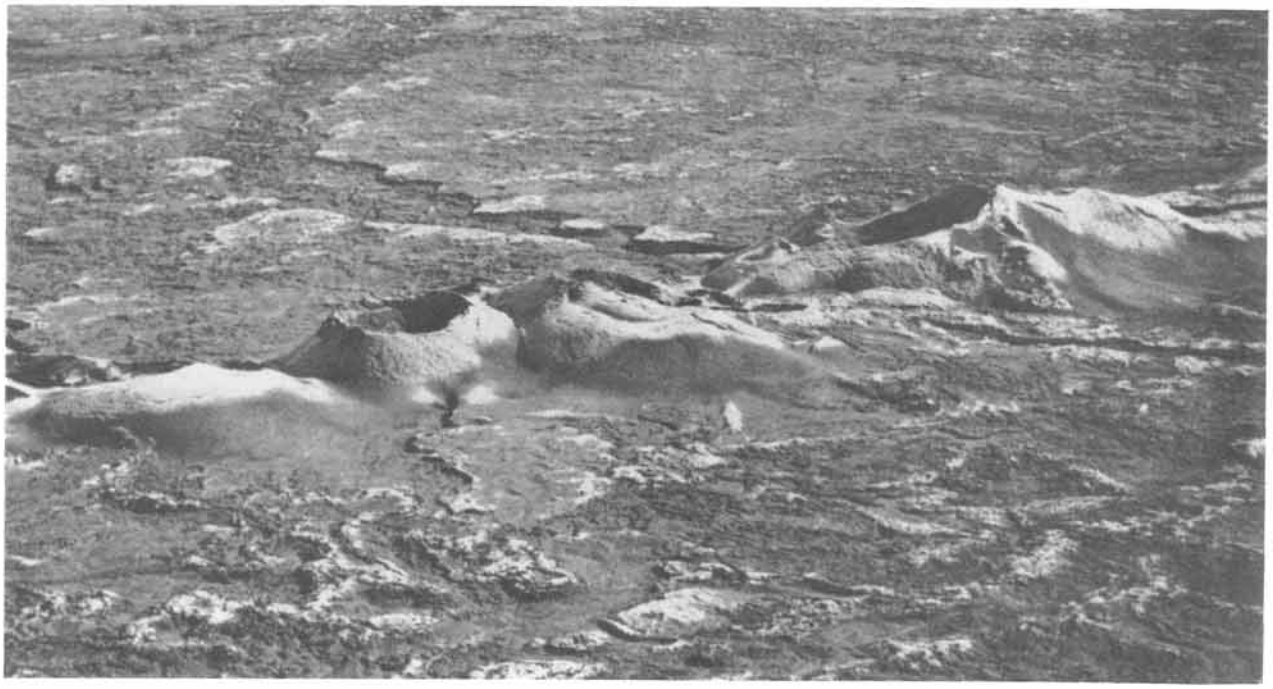

Figure 14-11a: *Cinder cones, formed in 1783, along part of the twenty-kilometer-long Laki fissure, Iceland.*

Figure 14-11b: *Aligned cinder cones of Harrat Kishb, Saudi Arabia.*

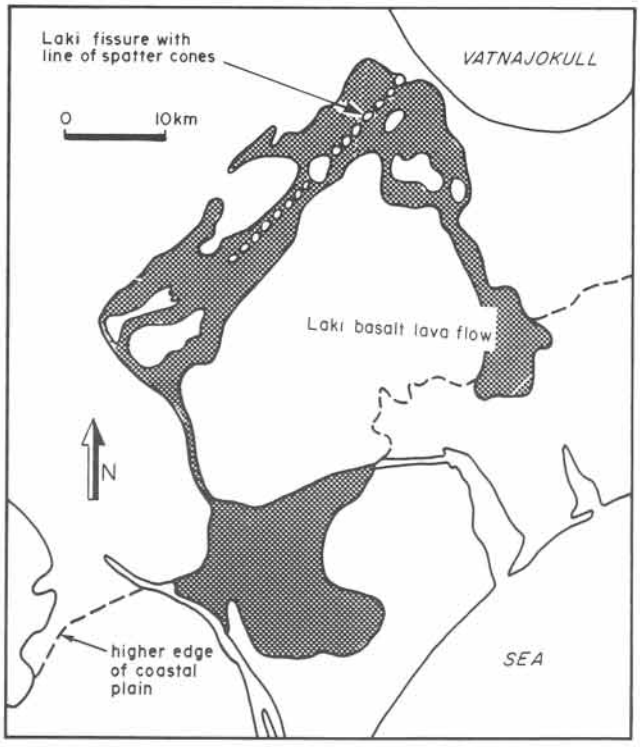

Figure 14-12a: *Map of the northeast-southwest trending Laki rift, showing the extent of the 1783 lava flood and the orientation of the cinder cones, Iceland.*

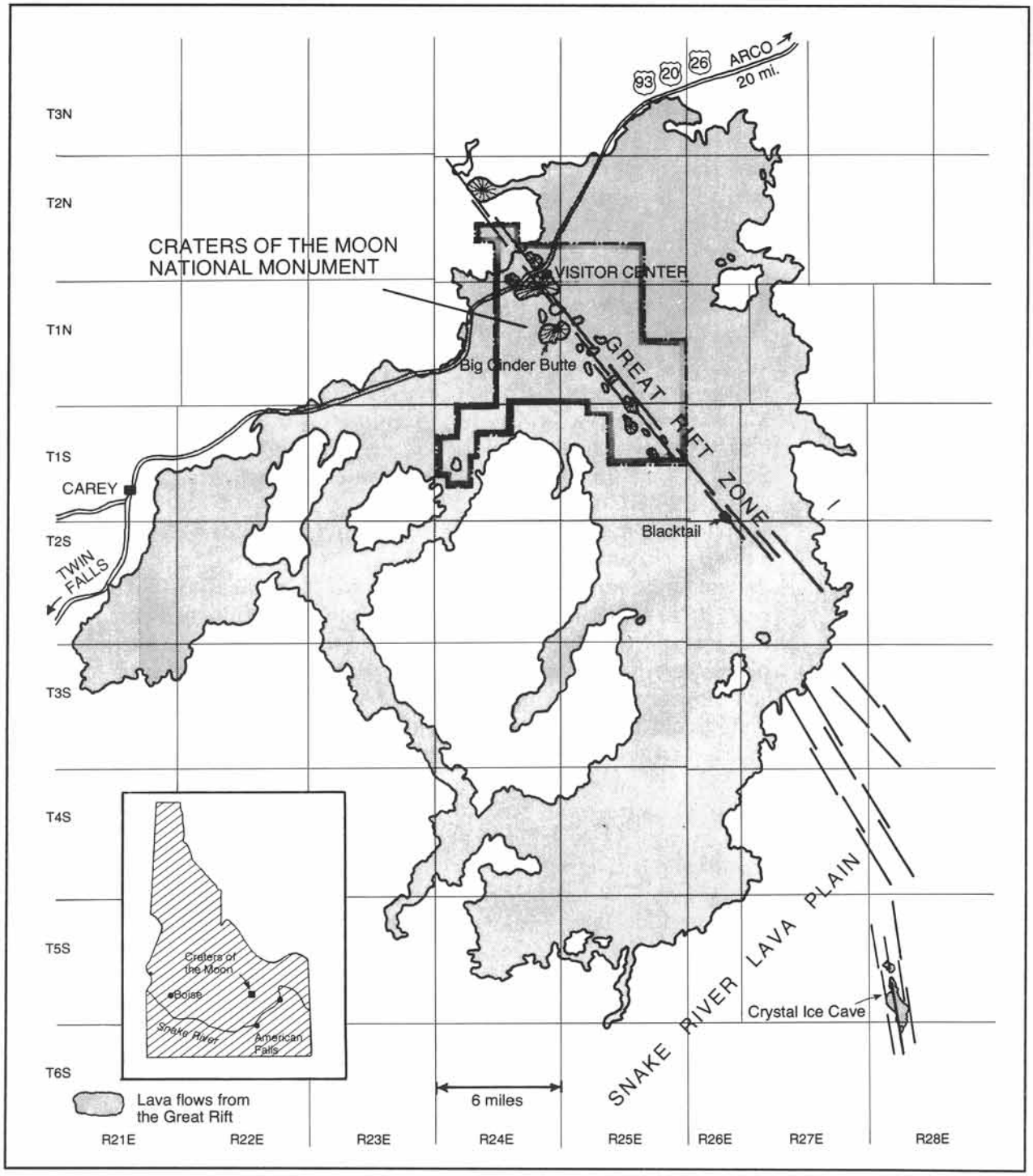

Figure 14-12b: *Map of the northwest-southeast trending Great Rift Zone, marked by cinder cones and the associated lava flows, Idaho. The cinder cones are part of the Craters of the Moon National Monument.*

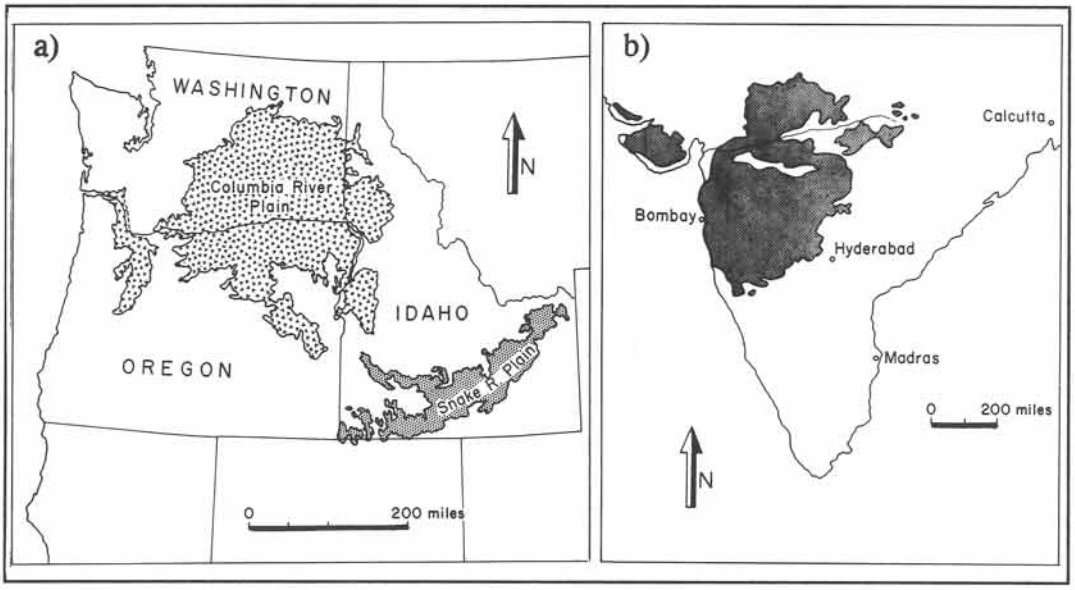

Figure 14-13: *a) Miocene flood basalts of the Columbia River Plateau, Washington. b) Cretaceous flood basalts of the Deccan traps, India.*

☐Exercise 14-1: Figure 14-14 is a schematic cross-section through a sequence of flood basalts. The succession includes shield volcanoes, feeder dikes, degraded cinder cones, erosion soils, and intercalations of continental sedimentary rocks. Discuss the geological history, implied by the section data.

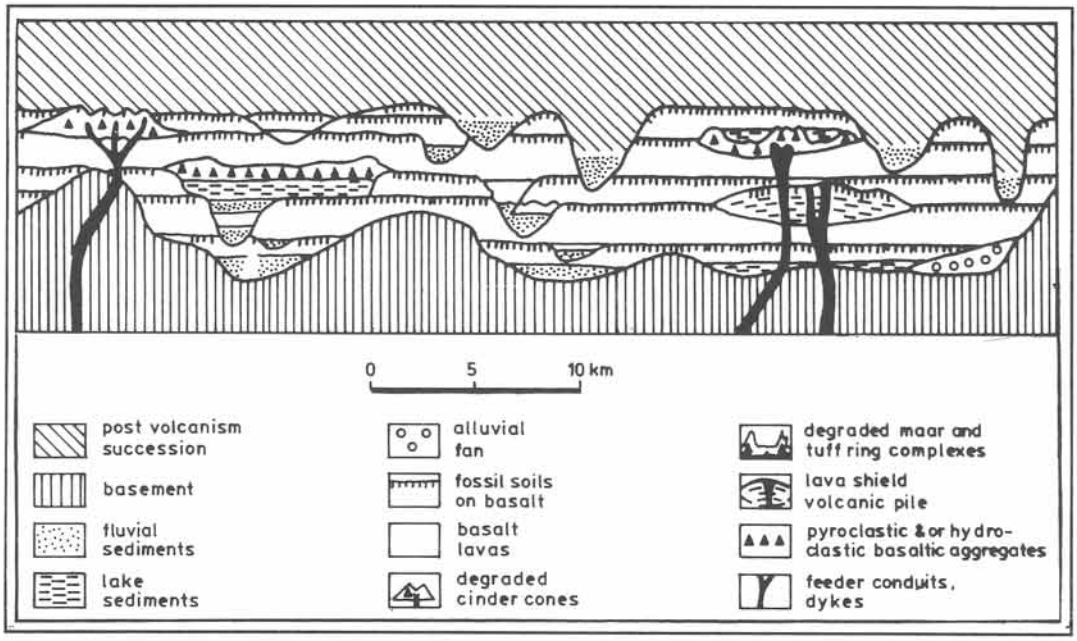

Figure 14-14: *Schematic cross-section of a flood basalt sequence. The vertical scale is of the order of one kilometer, and horizontal extent may be several hundred kilometers.*

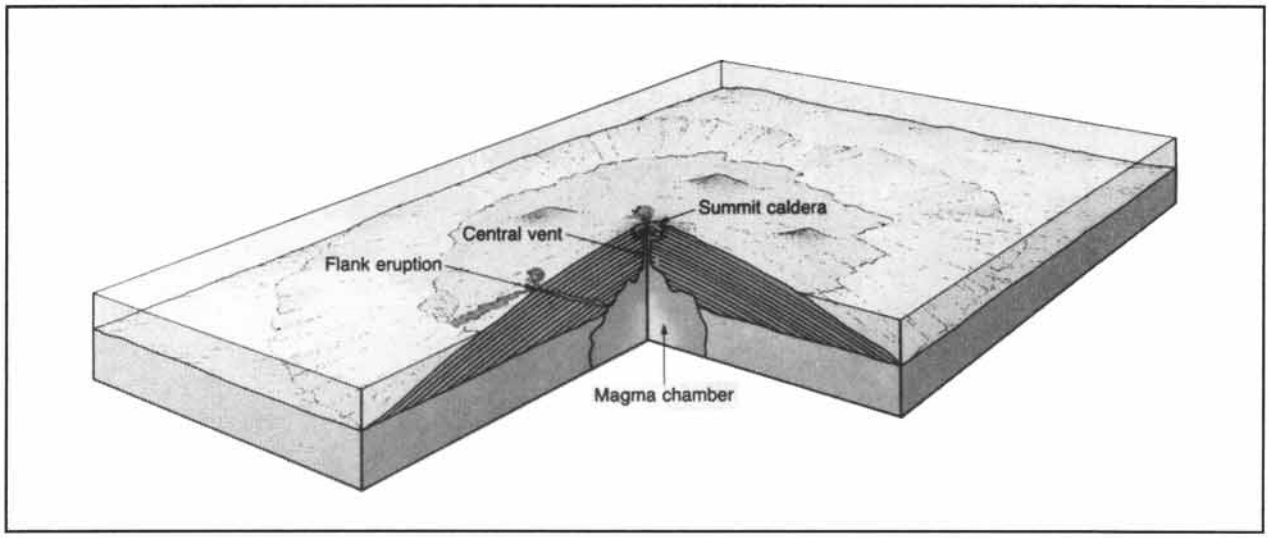

Figure 14-15: *Schematic perspective diagram of a shield volcano, built principally from stacked lava flows and only a small percentage of pyroclastics.*

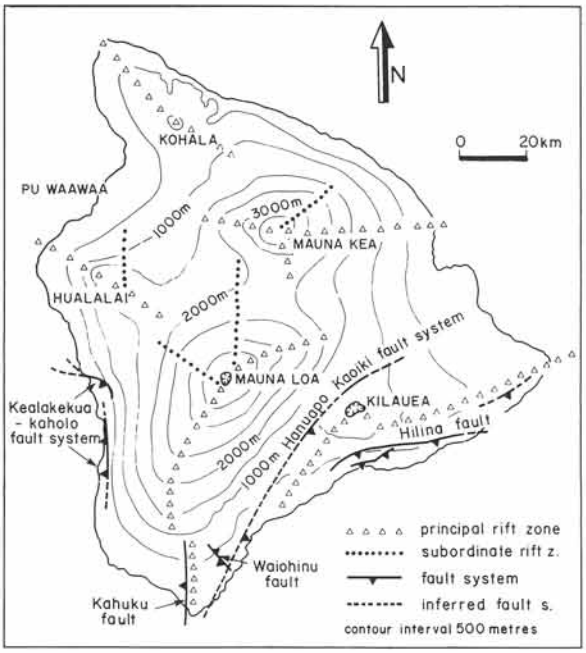

Figure 14-16: *The shield volcanoes of Hawaii; topographic contour map and location of the three principal shield centers, Mauna Kea, Mauna Loa, and Kilauea.*

14-4 Shield volcanoes

Rift zones and oceanic hot-spots may lead to the formation of basalt lavas, erupted from a single source. Basalt lavas have low viscosities and, therefore, spread out over large areas, forming shield volcanoes with width to height ratios of about ten (Fig. 14-15). *Shield volcanoes* contain few pyroclastic materials and are built up by successive lava flows accumulated by episodic eruptions over a time span of tens of thousands of years. The Kilauea volcano on the island of Hawaii has erupted over fifty times in recorded history. Mauna Loa, Hawaii's chief shield volcano, was built by eruption cycles, spanning about one million years (Fig. 14-16). The base of Mauna Loa rests on a five-kilometer-deep ocean floor, and its summit stands a full four kilometers above sea level. Most of the recent eruptions on Hawaii originate from linear fissures on the flanks of Mauna Loa (Fig. 14-17a to c). The Hawaiian Islands formed in a chain over a hot-spot. Movement of the Pacific plate has carried older shield volcanoes of this chain toward the northwest. Other examples of major shield volcanoes are Skalbreidur on Iceland and the Galapagos in the Pacific.

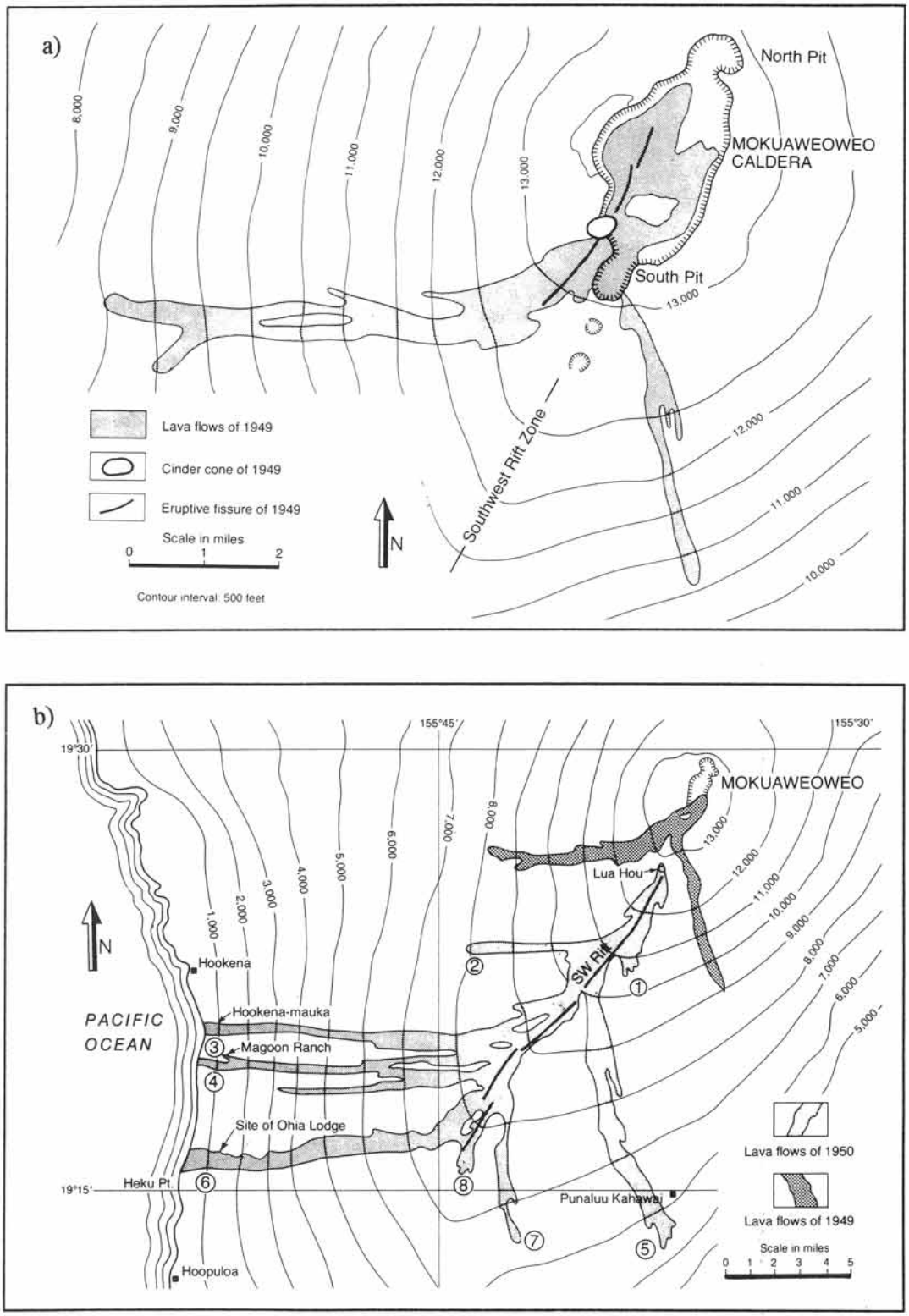

Figure 14-17: *Hawaiian fissure vents and associated lava flows on topographic base maps. a) Central rift in Mokuaweoweo collapse pit for 1949 flow. b) Southwest rift for 1950 flow.*

☐Exercise 14-2: Study the map of Figure 14-17c, and discuss the sequence of fissure eruptions that led to the eruption of the lava outbreaks, A to V, in chronological order.

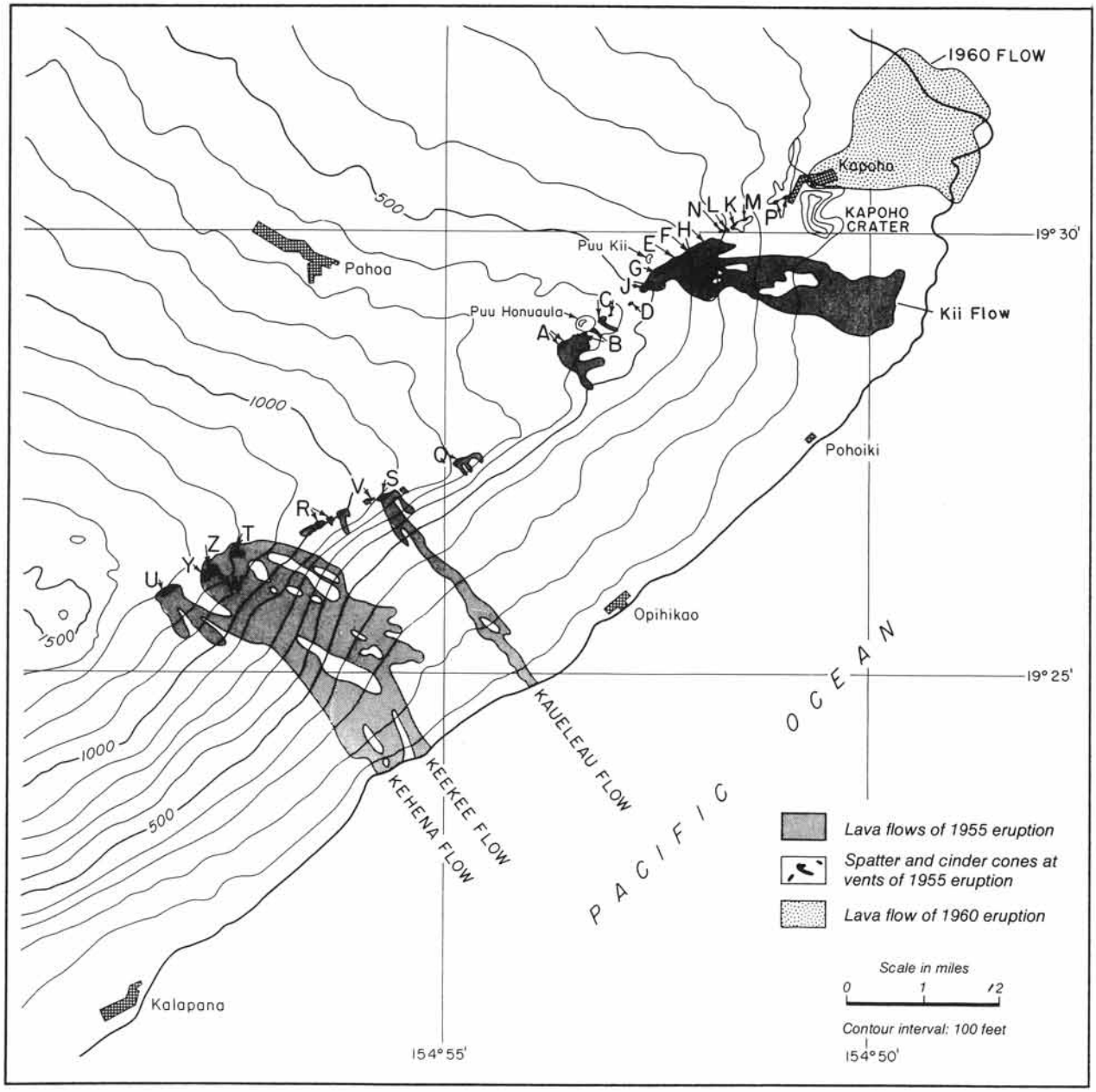

Figure 14-17c: *Rift zone east of Kilauea for lava flows of 1955 and 1960.*

14-5 Stratovolcanoes

The *stratovolcano* or *composite cone* is the archetype of the most abundant eruption cones (Fig. 14-18). Composite cones commonly form high mountains with concave slopes, contrasting with the convex shape of shield volcanoes. Fujiyama, on Japan's main island of Honshu, is a good example of a stratovolcano, rising up to nearly four kilometers high from a thirty-kilometer-wide basal diameter at sea level (Fig. 14-19a). Fujiyama lies on a line of active volcanoes on the Pacific plate, possibly representing a major fracture zone (Fig. 14-19b).

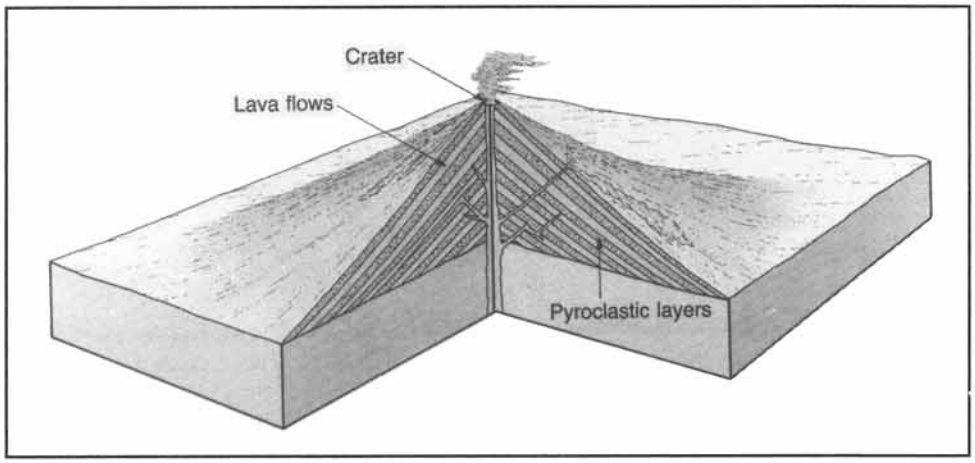

Figure 14-18: *Schematic perspective diagram of stratovolcano or composite cone, built of alternating layers of lava flows, epiclastics, and pyroclastics.*

Stratovolcanoes typically occur above slabs of oceanic lithosphere, descending into the mantle at active subduction zones. They frequently erupt, often explosively, and build stratovolcanoes from

Figure 14-19a: *Artistic representation of Mount Fuji (3776 m), Japan, with concave slopes characteristic of stratovolcanoes. Wood-block print by Hokusai - one of his thirty-six views of Mount Fuji.*

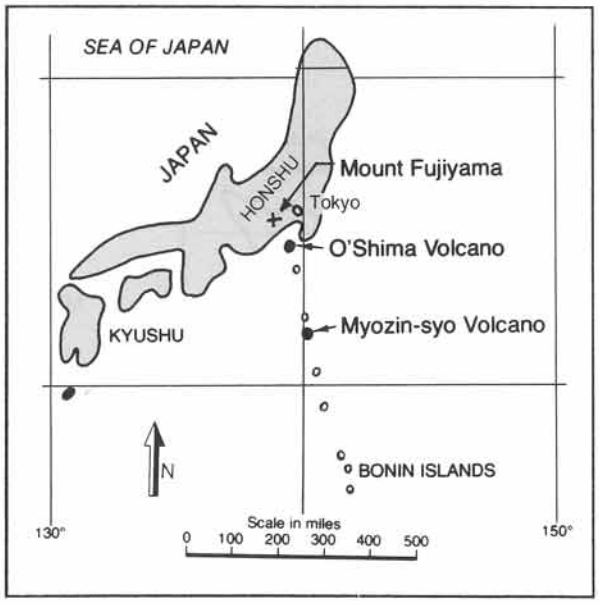

Figure 14-19b: *Location map of Mount Fuji and its alignment with volcanic islands off-shore.*

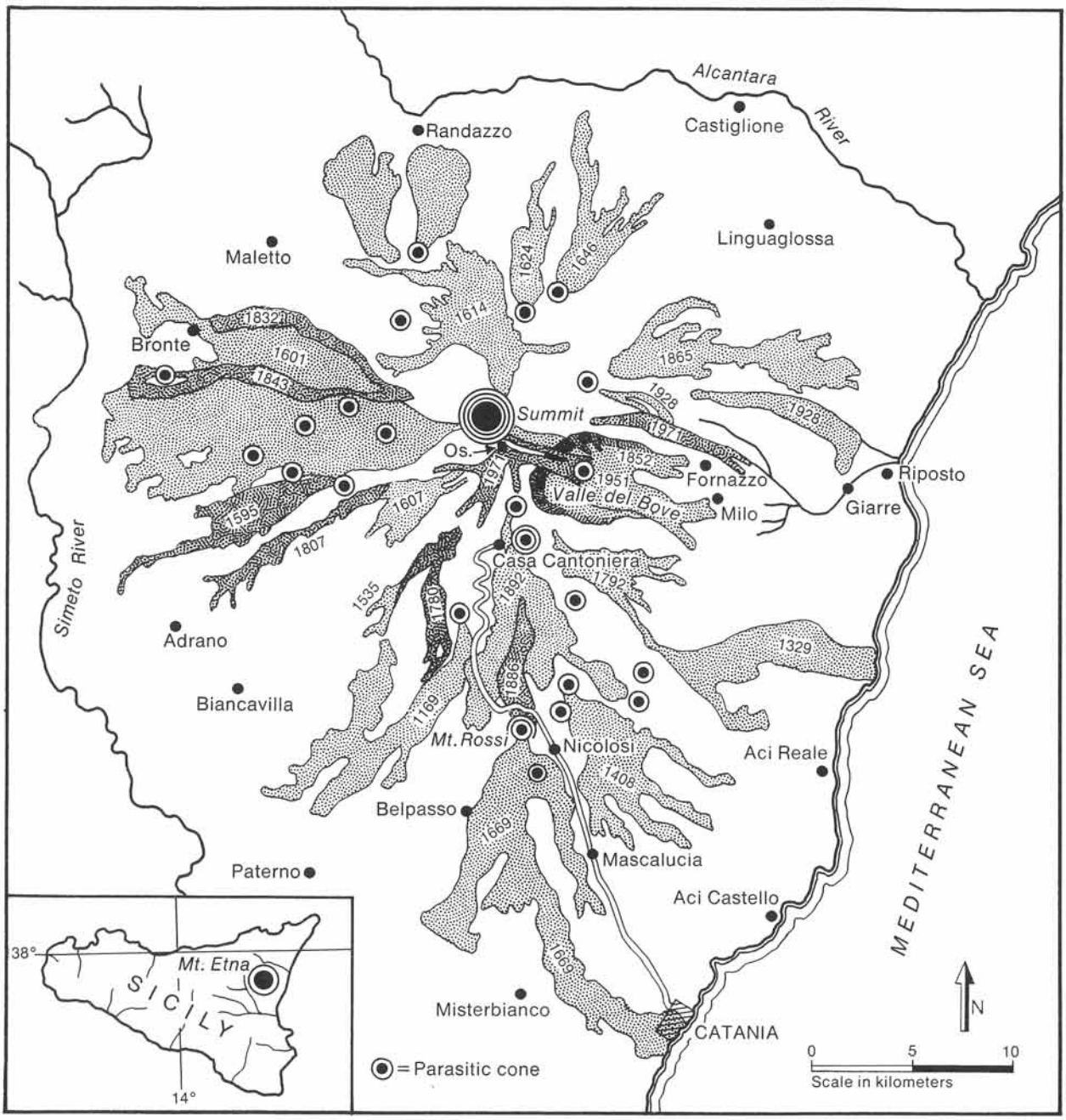

Figure 14-20: *Map of historic lava flows on Mount Etna, Sicily. The former volcanological observatory (marked: Os.) was destroyed during the 1991 eruption.*

interleafing layers of lava flows and pyroclastics. *Epiclastic deposits*, which consist of a mixture of rocks displaced by the eruption, are commonly encountered. The explosive character of stratovolcanoes originates from a higher water and gas content. The lavas erupting from them commonly contain a higher silica fraction than basic lavas. But no stratovolcano is wholly acid, because they, also, include basalt and andesite interstratified with acid lavas. Extreme compositions of stratovolcanoes occur in Mount Fuji (mainly basaltic) and Mt. Pelée (dominantly andesitic).

Figure 14-20 maps some of the principal lava flows observed at Mount Etna, Sicily, in recent history (1169-1971). Etna rises 3.5 kilometers above sea level and is extremely active. The most violent eruption in recent history occurred in 1669 and a fifteen-kilometer-long lava flow destroyed the city of Catania. It can be inferred that a volcano of Etna's size requires about one million years to build by episodic eruption of lavas and pyroclastics. The map pattern of the lava flows is chaotic and spreads away from the volcano summit. The detailed location of these lava flows is largely controlled by radial fissures, propagating from the summit downward.

Huge portions of the summit of mature stratovolcanoes may be blasted away after their slopes have become so steep that it is mechanically feasible to collapse them. The violent 1980 eruption of Mount St. Helens, Washington, was accompanied by massive sliding of its steep northern flank and a magnitude five earthquake (Fig. 14-21a to d). The slide lowered the volcano summit by about 400 meters, forming a two-kilometer-wide and 700-meter-deep breached crater. The sliding and summit collapse were triggered by increasing pore pressure, caused by expanding volcanic gases and magma, which lowered the frictional resistance of potential slide surfaces. Previous eruptions are known to have taken place from 1842 to 1857 and about 1,900 BC. The 1980 eruption caused 36 deaths, and 23 persons were reported permanently missing. Geologist David Johnston was killed by a pyroclastic flow, while monitoring the volcano more than nine kilometers away from the mountain peak. A significant number of casualties were caused by the debris-laden mudflows, rushing down the mountain slopes after the sudden melting of the snow and ice cover of Mt. St. Helens.

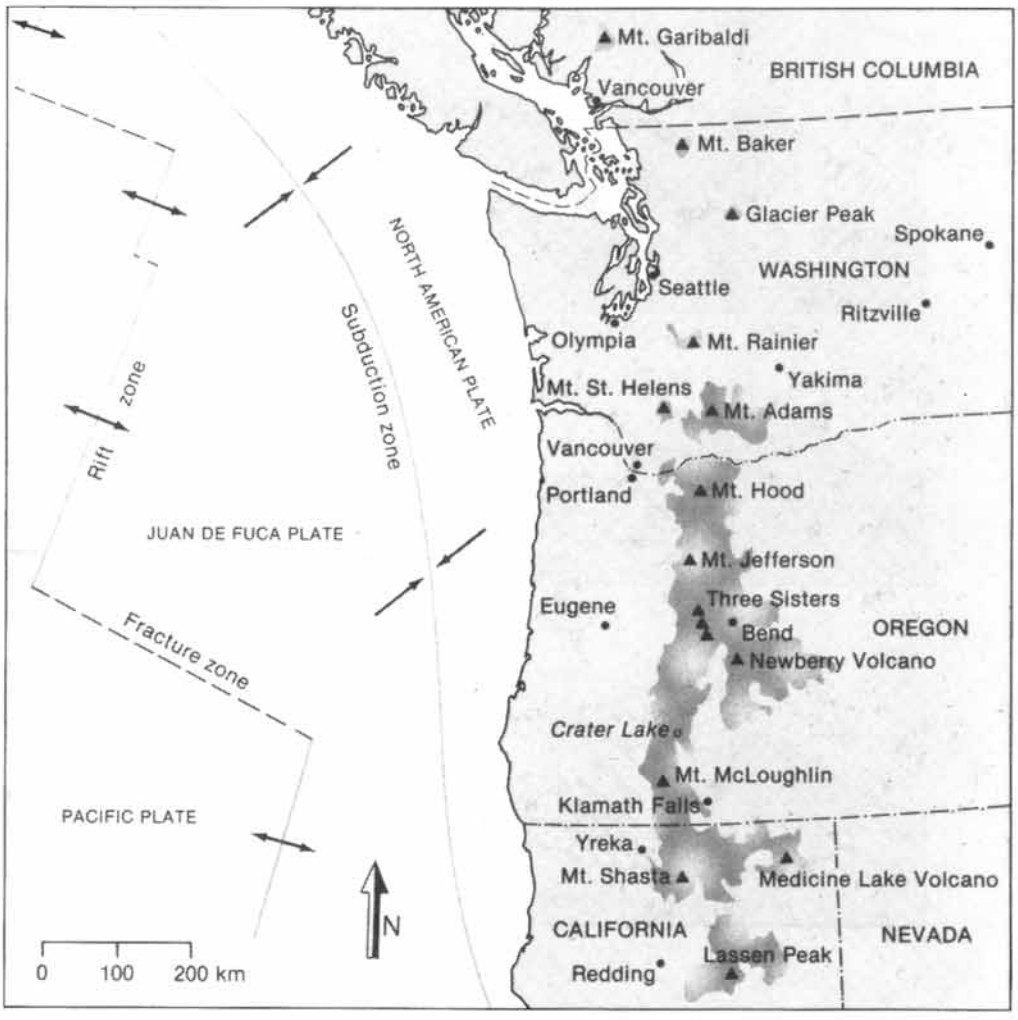

Figure 14-21a: *Location map of Mount St. Helens, Washington, and related volcanoes in the active belt of the Cascade Ranges. Dark-shaded areas are Quaternary extrusives.*

The violent eruptions of stratovolcanoes have claimed the majority of all human casualties and massive destruction related to volcanic activity. Some terrifying examples are: 30,000 deaths, caused by the glowing avalanche released during a 1902 eruption of Mount Pelée, Martinique; 16,000 deaths, caused by the 79 AD eruption of Mount Vesuvius, Italy; 36,000 deaths by ashfall and flood waves, set up by the 1883 eruption of Krakatao, Indonesia; 80,000 deaths by the famine, due to the 1815 eruption of Tambora, Indonesia, spoiling the crops; 25,000 deaths by mudflows from the 1985 eruption of the Nevado del Ruiz, Colombia.

☐Exercise 14-3: Estimate the length of transport involved in the displacement of the slide masses of the Mount St. Helens collapse.

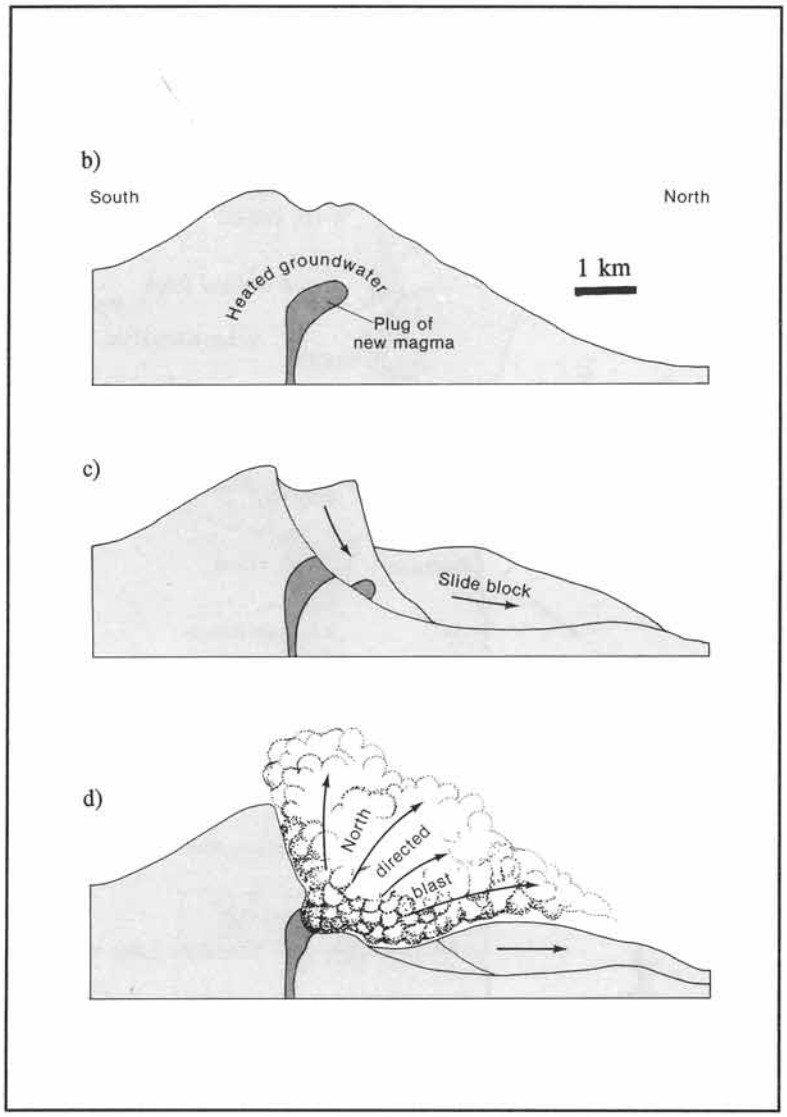

Figure 14-21: *b) to d) Collapse and sliding of Mount St. Helens during the violent 1980 eruption.*

14-6 Mudflows

The danger of *mudflows* or *lahars* (Indonesian) poses a serious hazard in volcanic terrains. They may be triggered by massive melting of ice caps following minor eruptions, by heavy rainfall that washes away unconsolidated deposits of recent ashfalls, or by overflowing of crater lakes by reactivation of dormant volcanoes. Mount Rainier, a dormant stratovolcano located about one hundred kilometers northeast of Mount St. Helens, is listed as a volcano likely to erupt before long. This more than four-kilometer-high volcano is largely covered by glaciers (Fig. 14-22a). Careful mapping has revealed the extent of two ancient mudflow deposits, i.e., the 500-year-old Electron mudflow and the 5,000-year-old Osceola mudflow (Fig. 14-22b). The Electron mudflow consists of 0.2 cubic kilometers; the Osceola flow has a volume of 2.5 cubic kilometers. The last eruption of Mount Rainier took place between 120 and 150 years ago. A map of potential hazards caused by a future eruption of Mount Rainier, published by the United States Geological Survey, outlines the risk areas for mudflows, lava flows, and ashfall (USGS map L-836 by D.R. Crandell, 1973).

Scarcity of volcanic hazard maps and poor public awareness still lead to tragedies, which might have been averted or limited if the potential dangers were better understood. In 1985, eruption of the Nevado del Ruiz volcano, Colombia, triggered mudflows. Several valleys were filled with mudflows, including the Lagunillas River, which buried the town of Armero, fifty kilometers away from the volcano summit. The mudflows reached speeds of forty to sixty kilometers per hour. Almost the entire population of 22,000 was either buried alive or drowned in muddy and debris-laden waters. The rampage was closely televised, with horrifying footage of failed attempts to rescue victims sinking away in the deep mud.

Geologists were aware of the potential danger posed by the dormant Nevado del Ruiz. Armero itself was built on the ruins of an earlier, 1845 mudflow, which had killed about 1,000 people. The delay between the 1985 eruption and the arrival of the mudflows in Armero was about two hours. However, there was no flood warning system - which is lacking in many regions of potential mudflow - and the population of Armero was taken by complete surprise.

☐Exercise 14-4: Order from your library or through interlibrary loan a copy of the USGS-Special Publication L-836. Study the hazard map, and discuss the merits of hazard control studies.

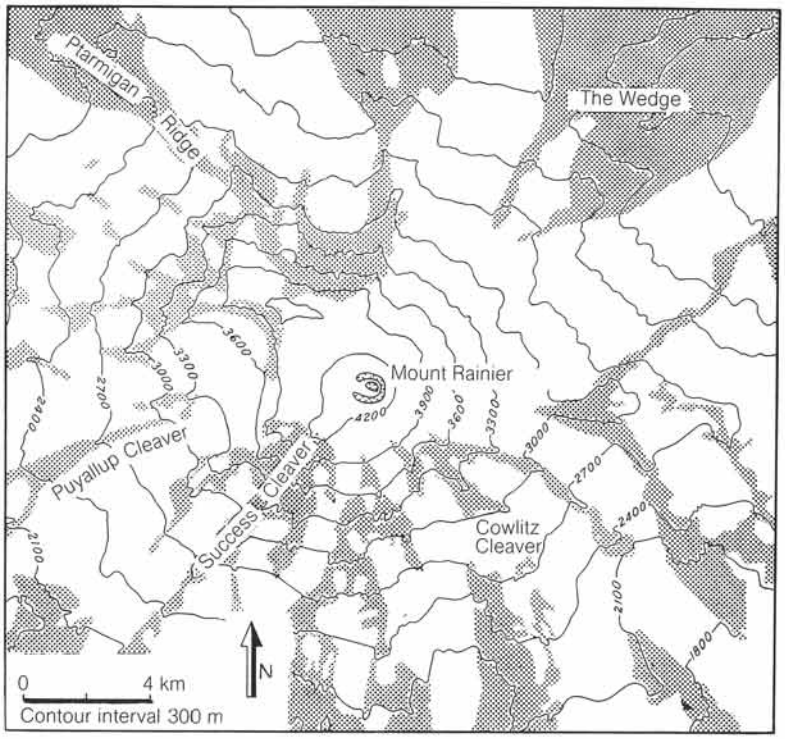

Figure 14-22a: *Topographic map of summit-area of Mount St. Rainier, Washington, marked with permanent glacier cover (white) and areas of bare rock (shaded).*

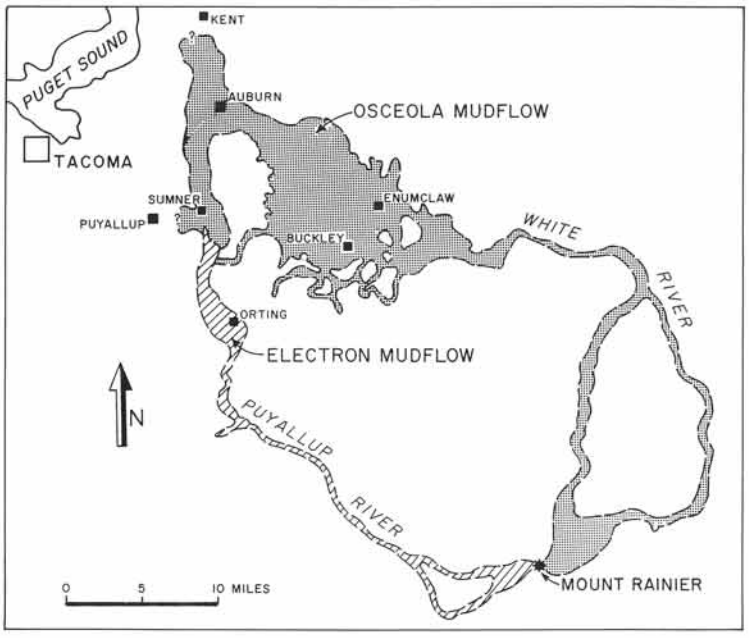

Figure 14-22b: *Regional map showing extent of the historic mudflows of Electron (500 years ago) and Osceola (5,000 years ago).*

14-7 Glowing avalanches

Apart from lava flows and mudflows, the eruption of stratovolcanoes is often accompanied by *glowing avalanches* or *nuée ardentes* (French). These are blasts of steam and hot gases, which engulf air and smoldering ejecta, consisting of rock fragments, lava bombs, and hot volcanic ashes. The resulting deposits, formed by the ejecta, range from ignimbrite, pumice, and tephra to felsic tuff, and block and ash deposits. For example, Mount Pelée erupted andesite domes and nuée ardente, which are filled with dense blocks of dome material.

The Roman city of Pompeii on the southern slope of the Vesuvius stratovolcano was struck by glowing avalanches in 79 AD, and subsequent ashfall buried the entire city in several-meter-deep pyroclastics (Fig. 14-23a & b). The city was forgotten and not rediscovered until about 1750. The excavation work now spans more than two centuries and is continuing at present. Numerous remains of persons and animals, trapped in the ashes, have been found in cavities formed by the ashes, which originally covered their bodies. Many of the cavities have been filled with gypsum, and the cured casts show the victims in agonizing positions (Fig 14-23c & d).

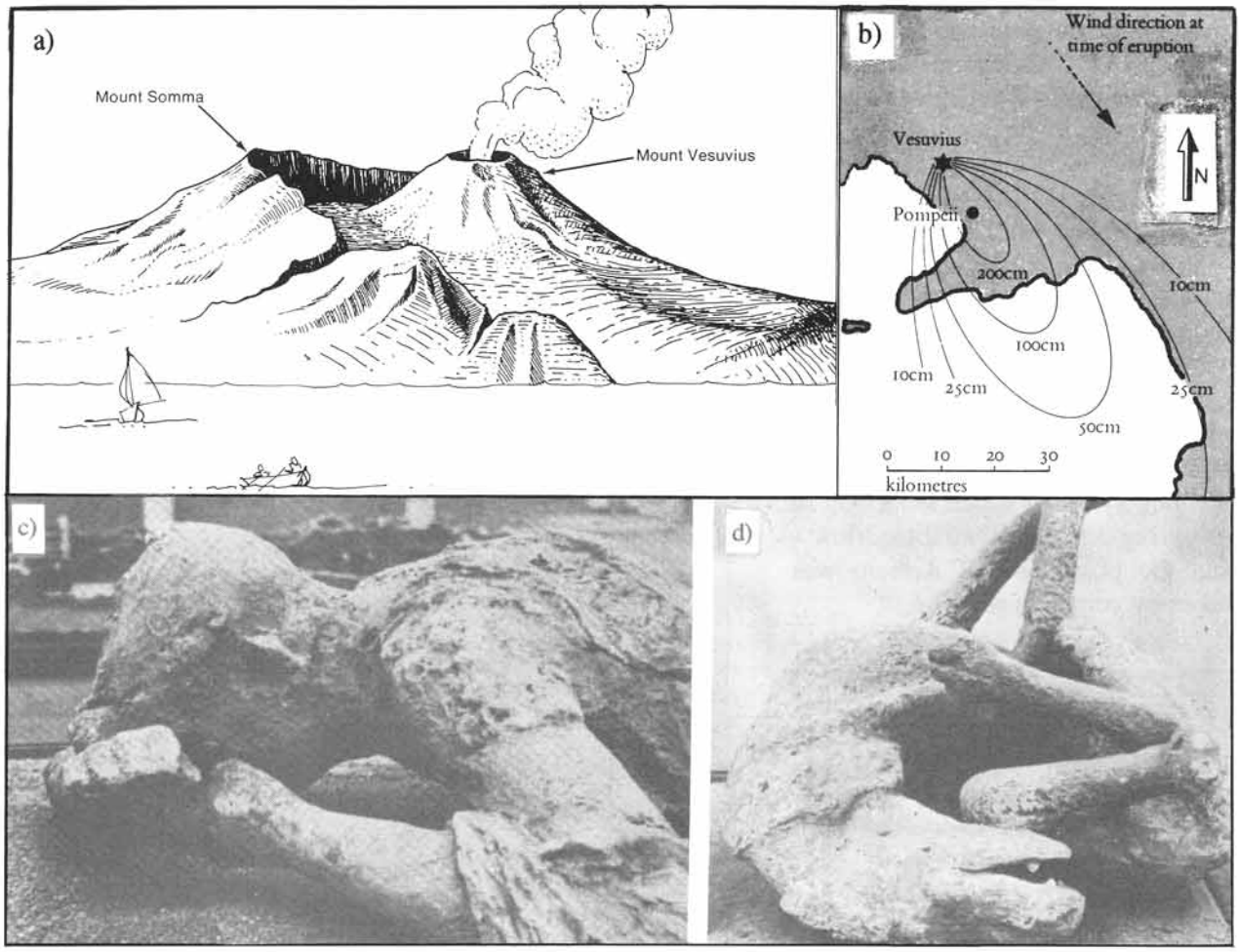

Figure 14-23: *Mount Vesuvius, Italy. a) Perspective view of Mount Vesuvius and its location within the caldera rim of Mount Somma. b) Isopach map of pyroclastics, deposited during the 79 AD eruption, which buried Pompeii. c) and d) Gypsum casts of victims of Pompeii (man and dog).*

The entire population of St. Pierre, Martinique, was killed by a nuée ardente, which flowed down from the erupting Mount Pelée in 1902 (Fig. 14-24a). Martinique is part of the volcanic island arc, located where the Caribbean plate overrides a subduction zone of Atlantic plate (Fig. 14-24b).

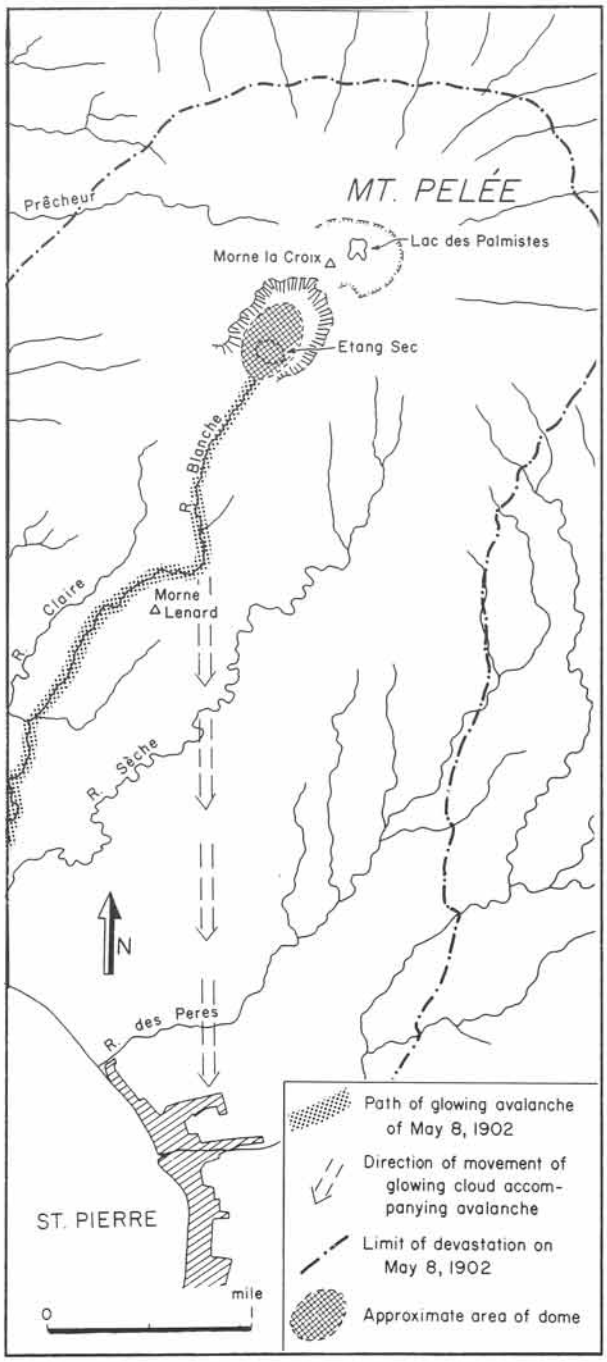

Figure 14-24a: Map of Mount Pelée, Martinique, and relative position of St. Pierre, hit by the nuée ardente of 1902.

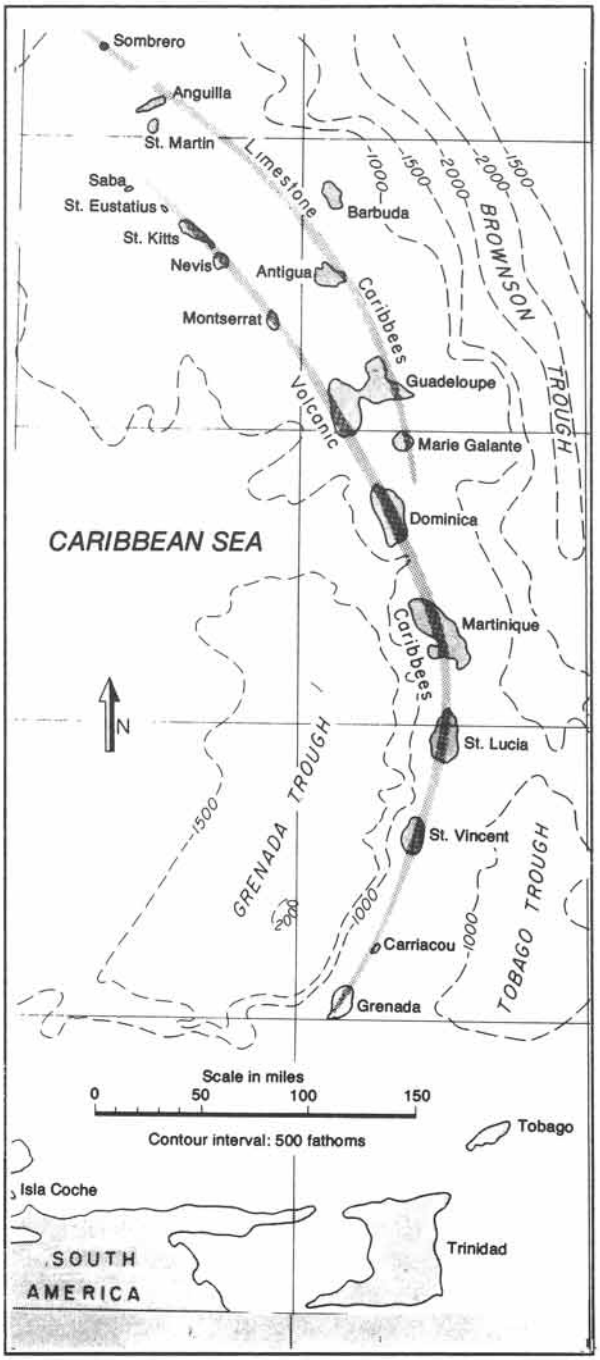

Figure 14-24b: Martinique is set within the volcanic island arc, which marks the leading edge of the Caribbean plate in the west overriding the subduction of the Atlantic plate in the east.

Figure 14-25: *Ruins of St. Pierre with Mount Pelée in the background, shortly after the glowing avalanche of May 8, 1902.*

The city of St. Pierre was actually destroyed by a surge of ash, which was part of a large pyroclastic flow over an area much wider than covered by the coarse, block-rich base of the flow. The nuée ardente collapsed thick masonry walls, uprooted large trees, and tore cannons from their mounts. The pressure wave capsized vessels moored in the harbor, and the hurricane of fire set ablaze the remaining ships. Only one out of eighteen vessels, the British steamship *Roddam*, managed to steam away with a dying crew, losing more than half of the men aboard due to burning and suffocation. The total destruction of St. Pierre was completed within a few minutes and left everything covered by a thin layer of smoldering volcanic ejecta (Fig. 14-25).

Figure 14-26 is a map of the Hibok-Hibok volcano, Camiguin Island, Philippines. An eruption in 1948 sent down mudflows, which destroyed part of Agoho village. A globule or dome of viscous lava started to grow in the summit of the crater early in 1949, episodically accompanied by explosions and minor glowing avalanches. However, massive nuée ardentes speeded down the slopes of Hibok-Hibok on 4 and 6 December, 1951 (Fig. 14-26). They killed about five hundred people in small villages southwest of Mambajao. The temperature of glowing avalanches reaches about seven hundred degrees centigrade, and they move fast, also. Glowing avalanches, emitted by Mount St. Helens, reached speeds of one hundred kilometers per hour.

The thickness of the ash deposits of the 79 AD Vesuvius eruption is dwarfed by the 1912 eruption of the Katmai volcano, Alaska (Fig. 14-27a). The isopach map of the ash deposits shows the maximum thickness reaches up to fifty feet close to the volcano proper (Fig. 14-27b). The explosive eruption took place at a vent at Novarupta, five kilometers west of the Mount Katmai summit. However, the massive release of ejecta from Novarupta was inferred to be coeval with caldera formation at Mount Katmai, lowering its summit by 400 meters and creating an oval depression of three to four kilometers wide and 600 meters deep. The area was not visited until several years after the eruption but was still fuming large quantities of white smoke, mostly escaping water vapor and gases (Fig. 14-28a). The director of the Katmai expeditions by the *National Geographic Society*, R.F. Griggs, termed it the Valley of Ten-Thousand Smokes. This ashfall deposit consists of pumiceous ash or *ignimbrite*, transported as a nuee ardente, which closely followed the topography of the terrain (Fig. 14-28b). The ignimbrite of the Valley of Ten-Thousand Smokes travelled a maximum distance of 22 kilometers from its source; ignimbrites have been mapped elsewhere at maximum distances of up to 225 kilometers from their eruption source.

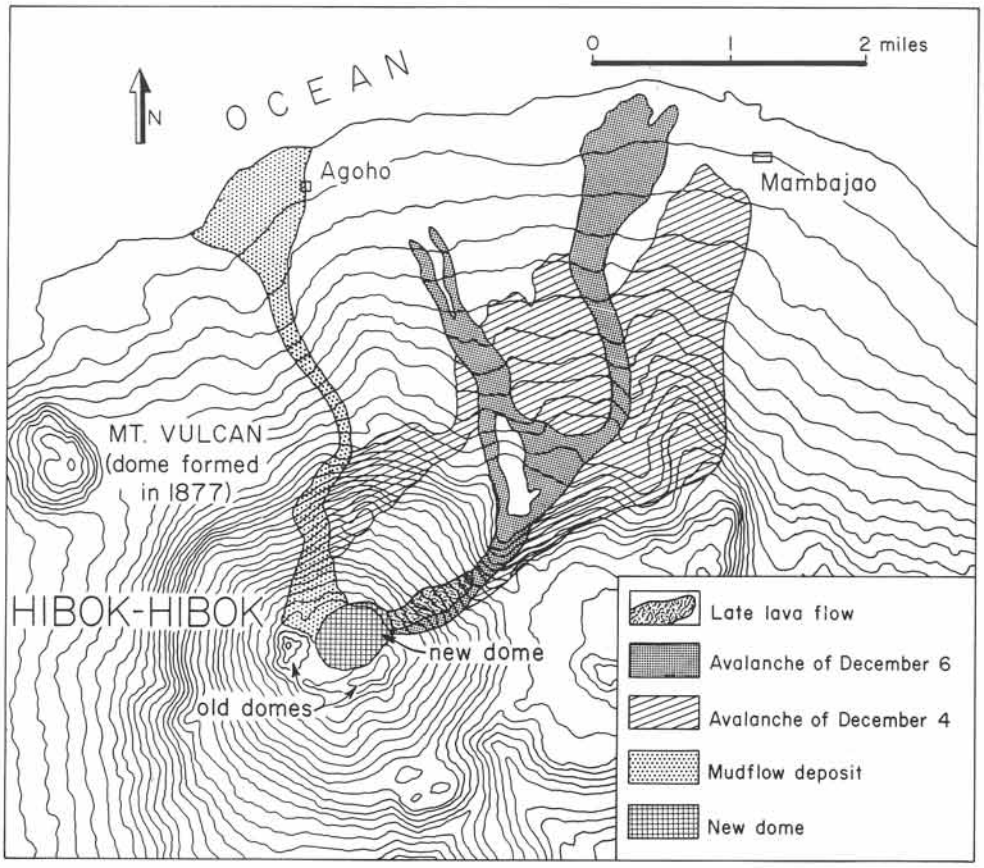

Figure 14-26: *Map of glowing avalanches and mudflows of Mount Hibok-Hibok, Camiguin Island, Philippines.*

Figure 14-27a: *Location map of Katmai volcano, Alaska.*

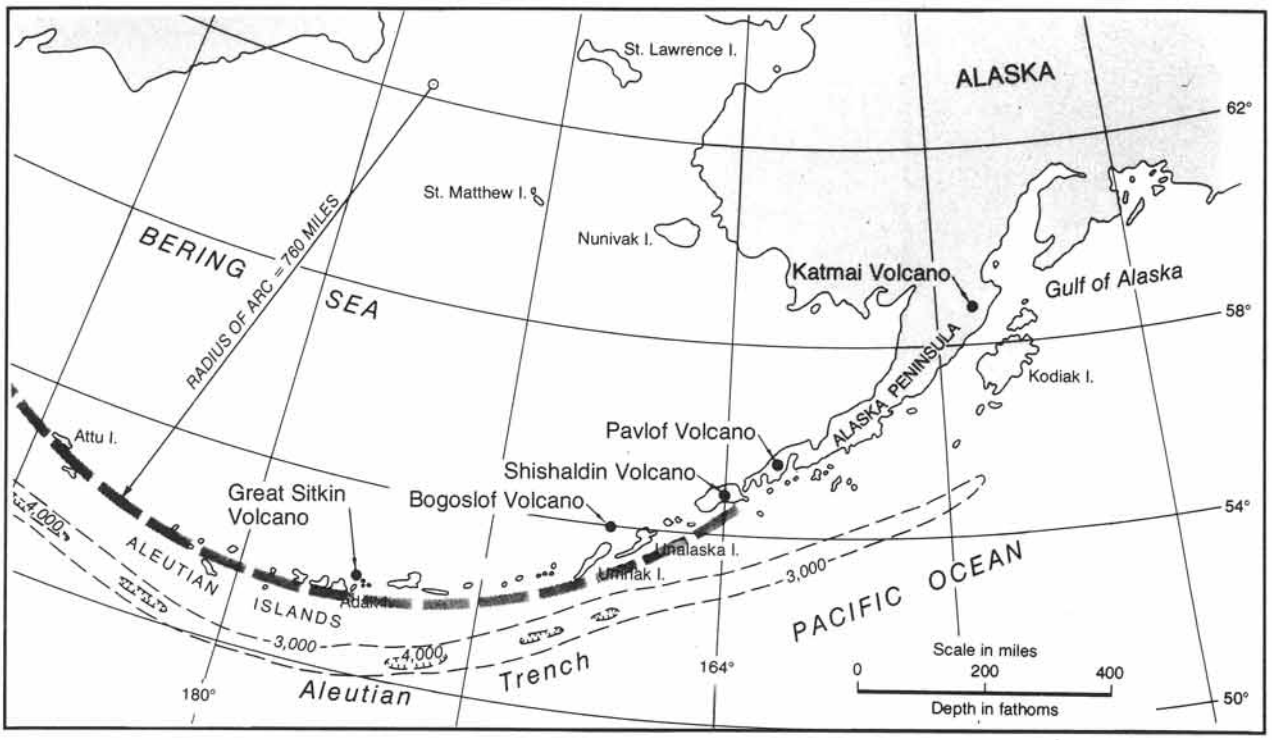

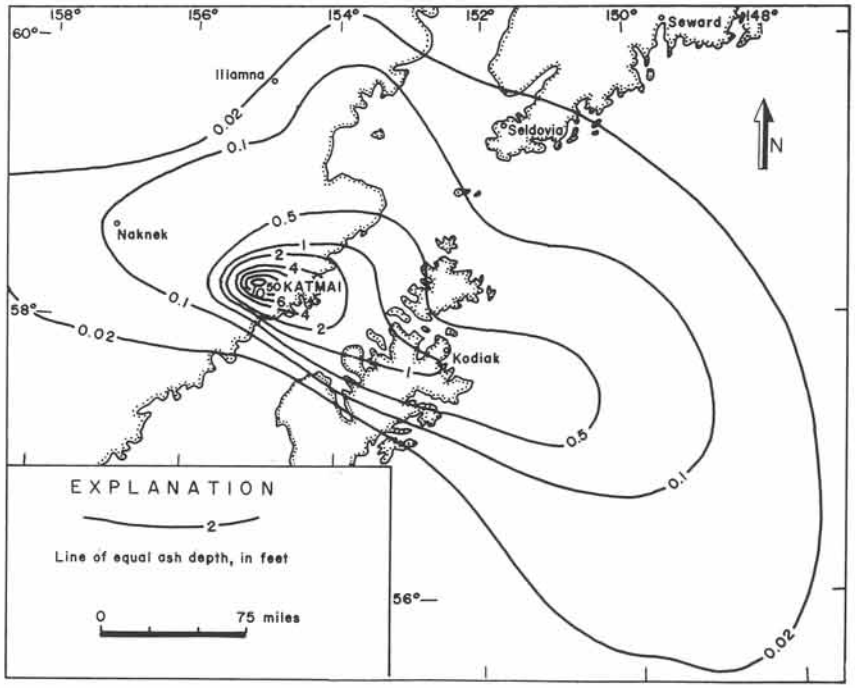

Figure 14-27b: *Isopach map for ash deposits of June 1912 eruption that created the Valley of Ten-Thousand Smokes.*

Figure 14-28: *Katmai volcano, Alaska. a) Valley of Ten-Thousand Smokes, as photographed by Griggs. b) Map showing the extent of the 1912 ignimbrite, associated with the glowing avalanche from the Novarupta vent.*

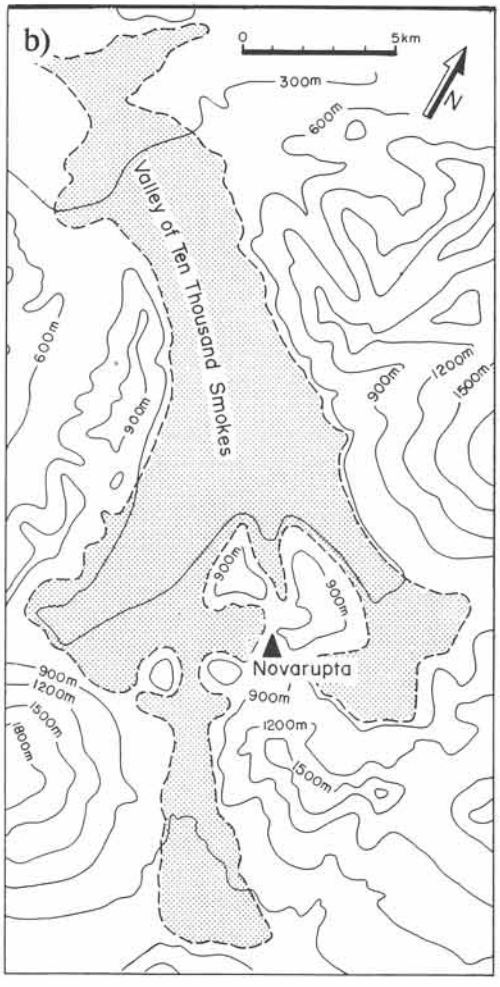

14-8 Craters and calderas

The collapse of Mount St. Helens, immediately prior to the May 18, 1980 eruption, was observed from a light aircraft about 400 meters above the summit. The gigantic, deep-seated landslide was an eye-opener and helps to understand better the historic disappearance of two major islands: Santorini and Krakatao.

A major island subsidence occurred about 1,500 BC in the volcanic archipelago of the Aegean Sea, Greece. The Minoan city of Akroteri, located on the flanks of the huge stratovolcano Santorini, suddenly subsided in a giant explosive eruption, accompanied by caldera collapse (Figs. 14-29a to c). The volume involved in the Santorini collapse is estimated at sixty cubic kilometers, more than three times larger than that of the Krakatao subsidence (see later). Santorini is considered one of the most likely locations for the legendary lost empire of Atlantis, which, according to Plato (427-347 BC), subsided into the ocean. The Santorini collapse must have been

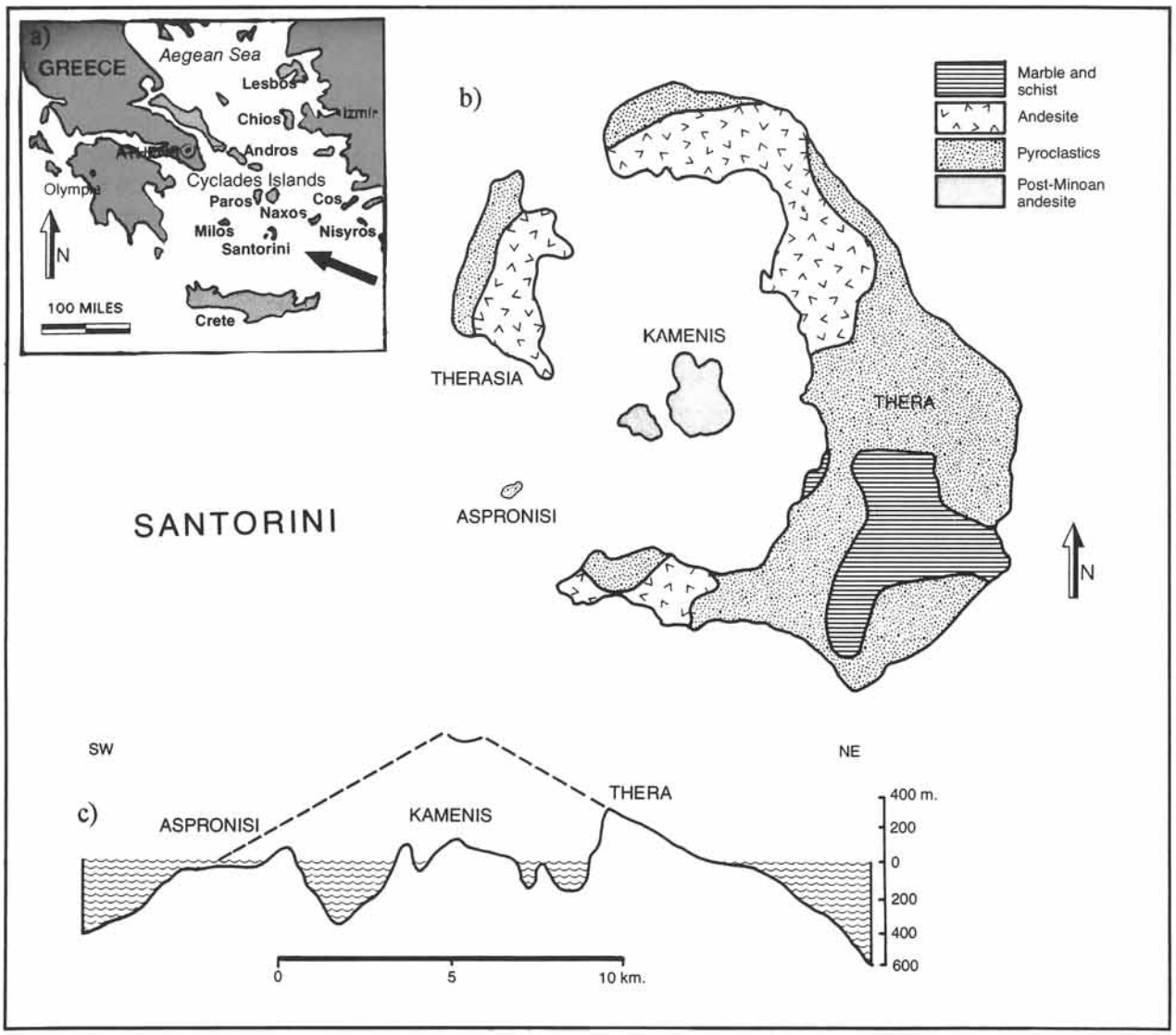

Figure 14-29: *Santorini volcanic complex, Aegean Sea, Greece. a) Location map. b) Geological map. c) Modern section and approximate outline of the volcano cone before its collapse, 1,500 BC.*

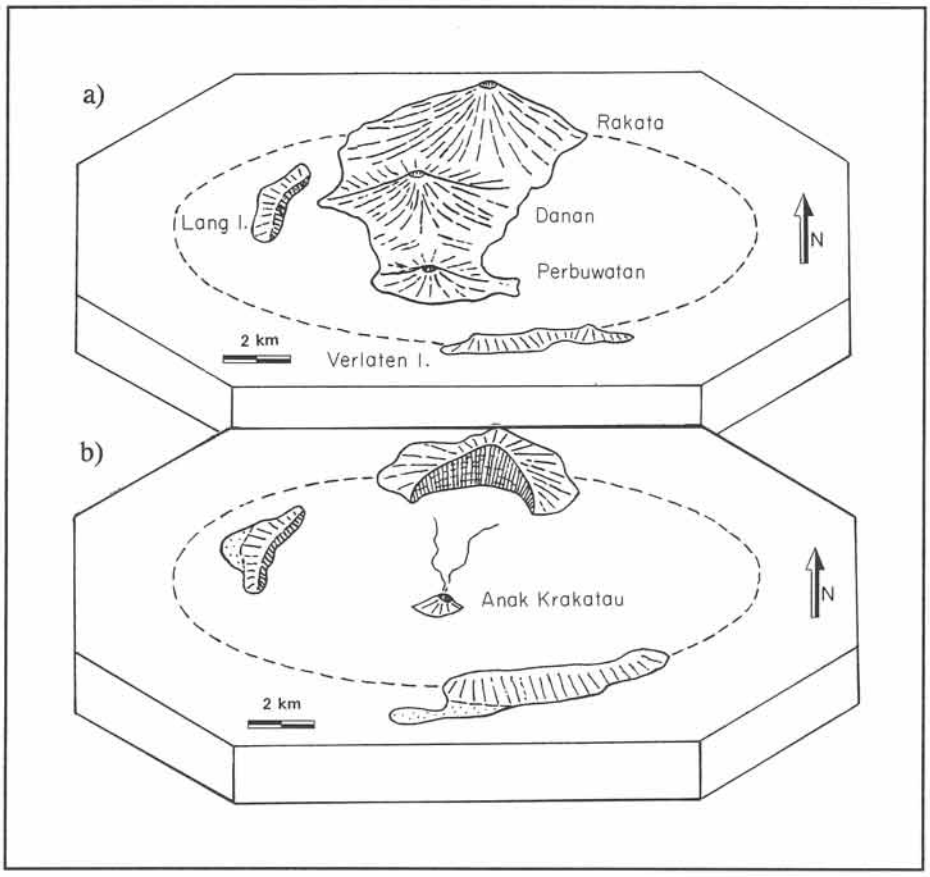

Figure 14-30: *a) & b) Perspective views of the Krakatao group before and after the eruption of 1883. Anak Krakatao, which emerged in 1930, is included.*

accompanied by a gigantic flood wave or *tsunami* (Japanese), and cities of the Minoan civilization on Crete, destroyed around 1,400 BC, are covered with pumice ashfall. Pumice layers of Thera, Santorini, have been excavated by French engineers to manufacture cement for construction of the Suez Canal. They uncovered man-made artifacts, which later were radiometrically dated at about 1410 BC (plus or minus 100 years). The Santorini volcano recovered by creating a new cone in the center of its collapsed caldera; the island of Kamenis rose in 197 BC with episodic additions until 1926. Incidentally, Wizard Island in Crater Lake, Oregon (section 13-3) is another example of a re-emergent volcano inside a caldera.

The main island of the Krakatao group, located in the Sunda Straits, Indonesia, almost completely vanished during an extremely violent eruption in 1883 (Figs. 14-30a & b). The rumbling explosion of the island was heard at thousands of kilometers distance. The 450-meter-high cone subsided in the blast and left the ground-floor 275 meters below sea level. The huge seismic tremors and submarine mass displacements caused a thirty-meter-high flood wave, which swept the coastlines of Sumatra and Java, killing 36,000 people (Fig. 14-31). It is not entirely clear whether the subsidence of Krakatao was due to lateral rock slides or vertical caldera subsidence or both. However, in 1930, volcanic eruptions pushed a new island above sea level (at the site of the formerly subsided volcano). It was appropriately named Anak Krakatao (Son of Krakatao). It now stands 200 meters high and measures nearly two kilometers in diameter.

The terms *caldera* and *crater* are somewhat mixed up in the literature, but for volcanologists they form by very different mechanisms. Craters result from outward explosion of debris and calderas by the inward subsidence of the volcanic superstructure into a partially erupted magma chamber. There is no hard rule about the field distinction, but, usually, calderas are defined as having diameters in excess of five kilometers, whereas craters are smaller than five kilometers in diameter. Volcanic subsidence features that

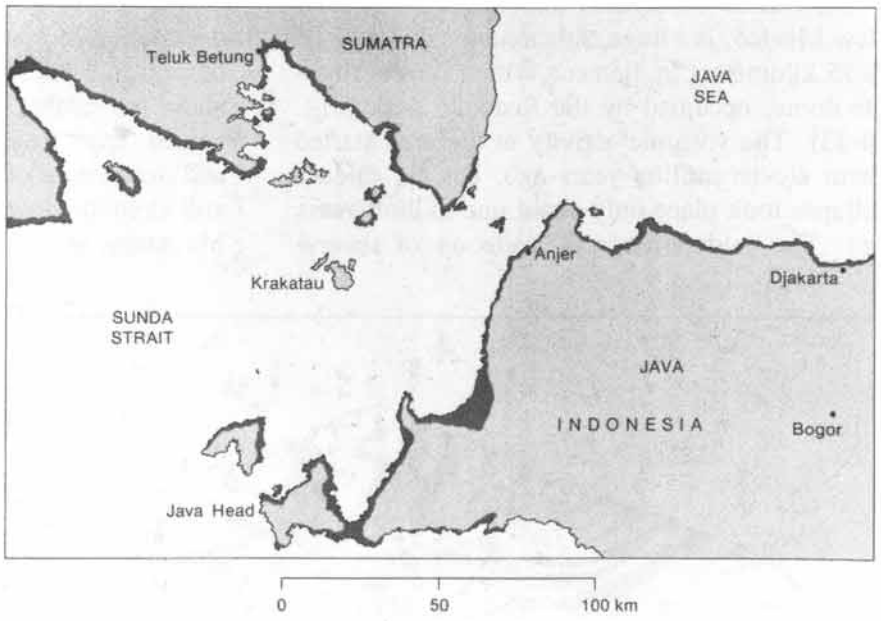

Figure 14-31: *Map of coastal area (shaded) inundated by tsunamis, originating from the 1883 collapse of Krakatao, killing an estimated 36,000 people.*

are less than five kilometers in diameter are termed *pits*. For example, the summit of Mauna Loa, Hawaii, hosts the Mokuaweoweo and several other, smaller *collapse pits* (Fig. 14-32).

☐Exercise 14-5: Calculate the volume (cubic kilometers) involved in the collapse of a volcano summit, which reduces its height by 300 meters. The slope of the original summit cone was 30°. Use the simple cone formula $V=\pi R^2h/3$, with base radius R and height h. Also, give an equation, expressing the volume in terms of height and slope, α, only.

Figure 14-32: *Oblique aerial view northward over the collapse pits of Mauna Loa, Hawaii. The summit of Mauna Kea appears in the background.*

The Valles Caldera in the Jemez Mountains, New Mexico, is a huge, subcircular caldera of 12 to 15 kilometers in diameter with a central rhyolite dome, occupied by the Redondo peak (Fig. 14-33). The volcanic activity in the area started about eleven million years ago, but the caldera collapse took place only about one million years ago. The caldera floor is made up of several jostled and tilted cauldron blocks, in between which new eruptions formed a dozen rhyolite domes. The caldera walls stand about 700 meters above the caldera floor. The volcanic activity has ceased, apart from the fuming of some solfatares and occurrence of hot springs. The welded tuffs and rhyolite flows on the slopes of the Jemez Mountains are developing inverted relief.

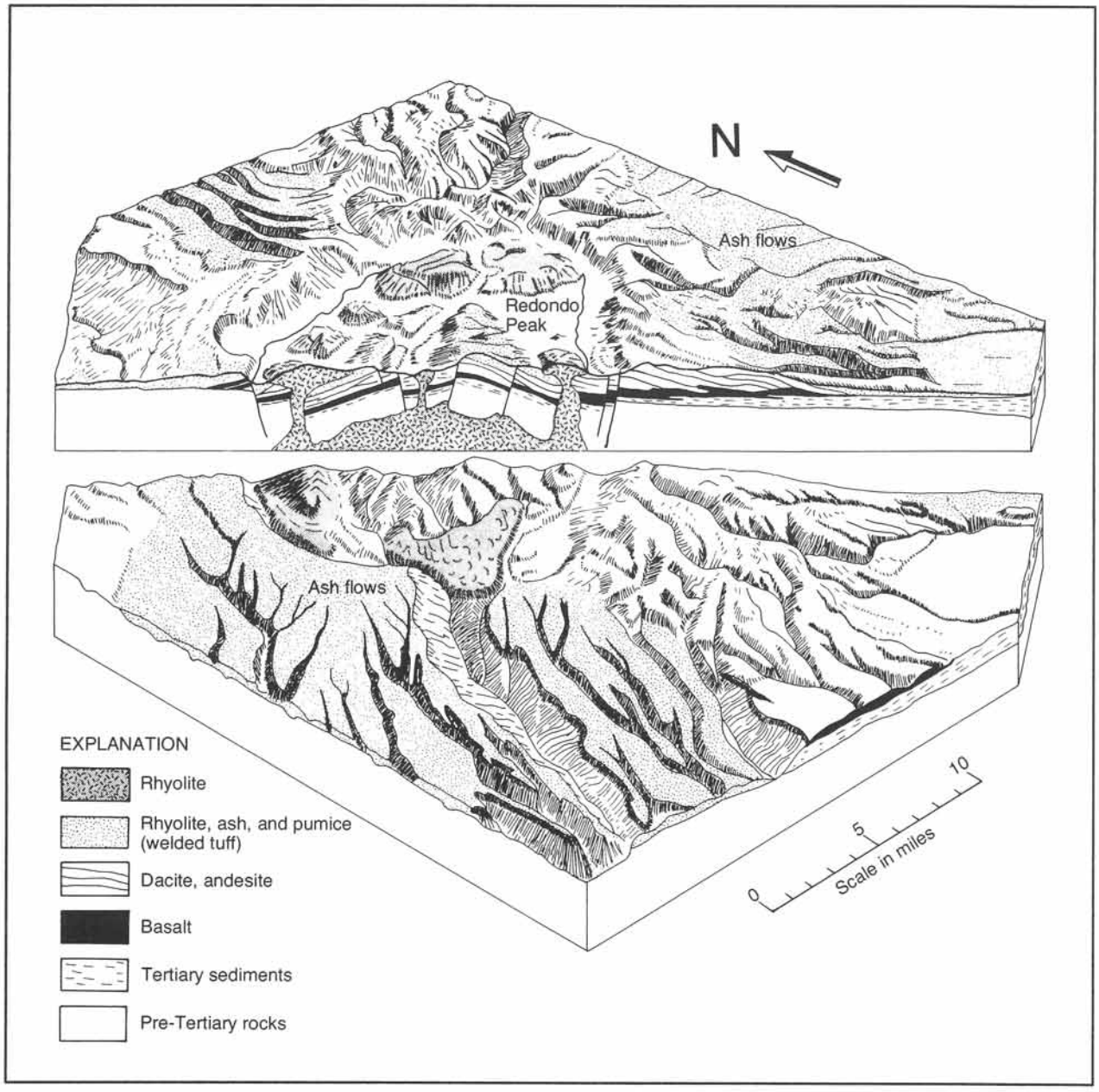

Figure 14-33: *Volcanic complex of Valles Caldera, Jemez Mountains, New Mexico.*

14-9 Eroded extrusives

Erosion slowly changes the relief and removes material from terrains with igneous extrusives. Figures 14-34a and b illustrate the change of a volcanic landscape after extensive erosion. The volcano cone is eroded away. All that remains in the landscape is a *volcanic neck*, the central feeder pipe of the former volcano. Shiprock Mountain, New Mexico, forms a magnificient example of such a volcanic neck. Shiprock towers some 400 meters above the surrounding desert plain with radial ridges, formed by dikes, emanating from the central stock (Fig. 14-34c). Lava sheets, if more

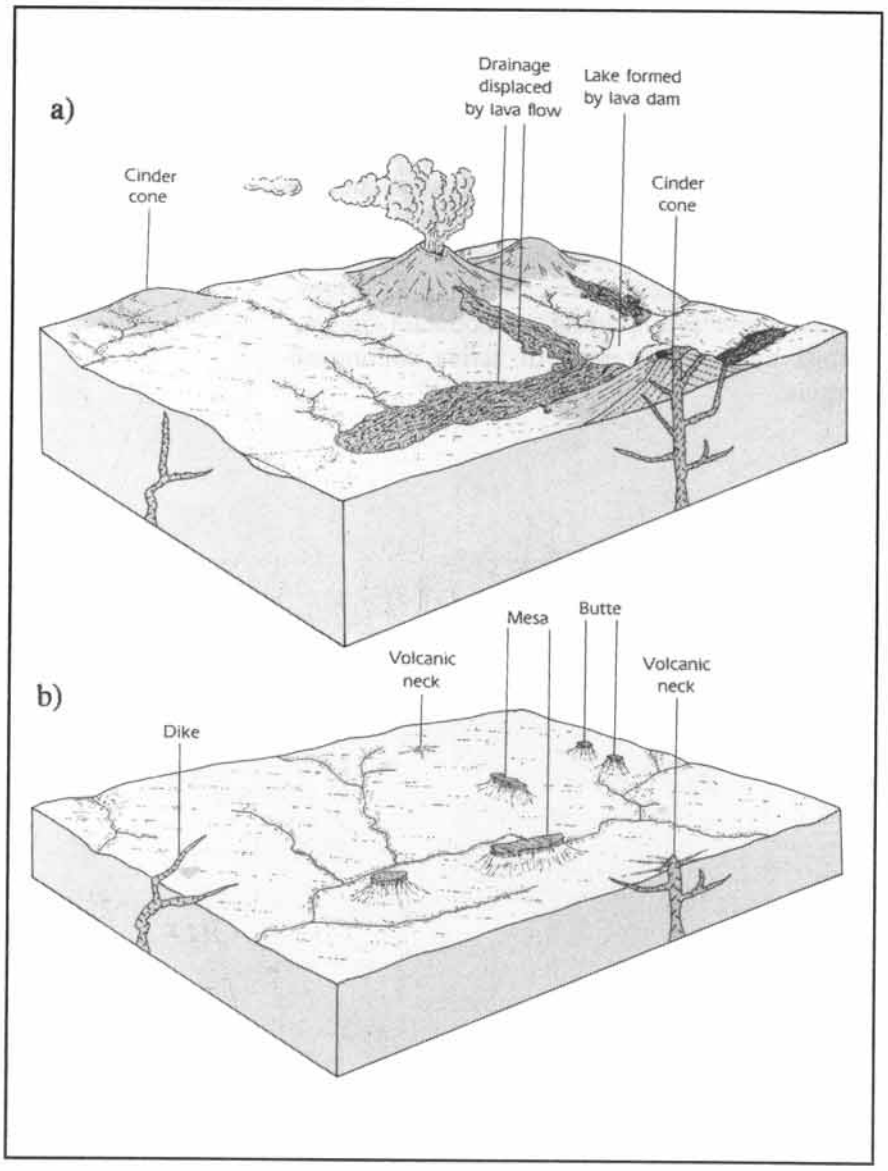

Figure 14-34: *Perspective diagram of volcanic landscape: (a) before, and (b) after, erosion. c) Shiprock Mountain, New Mexico, provides a spectacular example of a volcanic neck and radial dikes.*

resistant to erosion than the adjacent rock formations, may protect the underlying rocks from eroding away, thus forming an inverted relief. Former valleys, followed by the lava streams, are turned into *mesas* and *buttes*, elevated above the surrounding plains. Ultimately, the mesas, necks, and some dikes are all that remain of the volcanic structures. The erosion is particularly rapid in volcanic provinces above subduction zones, because these are uplifting as mountain ranges, formed by the thickening of active continental margins.

☐Exercise 14-6: Sketch two speculative map views, showing what the Valles Caldera region may look like (a) five million, and (b) fifty million years from now.